

The rotation-activity relation of M dwarfs: From *K2* to *TESS* and *PLATO*

St. Raetz^{1,*}, B. Stelzer^{1,2}, and A. Scholz³

¹ Institut für Astronomie und Astrophysik Tübingen (IAAT), Eberhard-Karls Universität Tübingen, Sand 1, D-72076 Tübingen, Germany

e-mail: raetz@astro.uni-tuebingen.de

² INAF - Osservatorio Astronomico di Palermo, Piazza del Parlamento 1, I-90134 Palermo, Italy

³ SUPA, School of Physics & Astronomy, University of St. Andrews, North Haugh, St. Andrews KY 16 9SS, UK

The dates of receipt and acceptance should be inserted later

Key words stars: late-type — stars: activity — stars: rotation — stars: flare

Studies of the rotation-activity relation of late-type stars are essential to enhance our understanding of stellar dynamos and angular momentum evolution. We study the rotation-activity relation with *K2* for M dwarfs where it is especially poorly understood. We analyzed the light curves of all bright and nearby M dwarfs from the Superblink proper motion catalog that were in the *K2* field of view. For a sample of 430 M dwarfs observed in campaigns C0-C19 in long cadence mode we determined the rotation period and a wealth of activity diagnostics. Our study of the rotation-activity relation based on photometric activity indicators confirmed the previously published abrupt change of the activity level at a rotation period of ~ 10 d. Our more than three times larger sample increases the statistical significance of this finding.

© 2006 WILEY-VCH Verlag GmbH & Co. KGaA, Weinheim

1 Introduction

Stellar activity is directly linked to magnetic fields that are believed to be generated and maintained by a dynamo which is driven by differential rotation and convection. Therefore, rotation and stellar activity are intimately connected.

The rotation-activity relation of late-type stars based on the measurements of the X-ray luminosity is empirically divided in two regimes: a “saturated” plateau of constant activity for fast rotators and a “correlated” regime for slow rotators. Because of the long spin-down times of M dwarfs compared to solar-like stars, rotation periods can become very long, depending on mass and age of the M dwarf (Scholz et al. 2013, Bouvier et al. 2014). Hence, for evolved, early M dwarfs, the long rotation periods and faint X-ray emission make the rotation-activity relation notoriously poorly defined.

By combining periods from the *K2* mission with archival X-ray data Stelzer et al. (2016) started towards providing a statistical sample of bright and nearby M dwarfs with both known rotation period and X-ray detection. Photometric observations with space telescopes such as the *K2* and *TESS* missions provide not only rotation periods even with low amplitudes but also a wealth of other activity diagnostics. The study of the rotation-activity relation based on photometric activity indicators by Stelzer et al. (2016) revealed, that, at a critical rotation period of ~ 10 d, the activity level changes abruptly. This drastic behavior is very different compared to the slowly decaying activity level seen in the corre-

lated regime of the X-ray luminosity of M dwarfs (Wright, & Drake 2016; Stelzer et al. 2016; Wright et al. 2018) or other activity indicators e.g. H_{α} (Newton et al. 2017). This phenomenon represents an open problem within the framework of dynamo theory.

NASA’s *K2* (*Kepler* Two-Wheel) mission was a space telescope dedicated for optical photometric monitoring. It was the follow-up project of the main *Kepler* mission after the failure of the second of four reaction wheels that were essential to maintain a very precise and stable pointing. The “Second Light” of *Kepler*, the *K2* mission which used a different observing concept, started its science observations in 2014 March (Howell et al. 2014). Until the end of the mission due to fuel exhaustion in 2018 October, *K2* observed series of sequential observing “Campaigns” (campaign duration ~ 80 d) of fields distributed around the ecliptic plane. *K2* provided continuous high precision light curves (LCs) in two cadence modes. The long cadence observations (~ 30 min data point cadence) was the default observing mode while short cadence LCs (~ 1 min data point cadence) were only provided for selected targets.

Stelzer et al. (2016) presented results for the relation between stellar rotation period and photometric activity indicators for a sample of 134 bright and nearby M dwarfs observed with the *K2* mission in long cadence mode during campaigns C0-C4. Here we present the extension of this study to all bright and nearby M dwarfs from the Superblink proper motion catalog (Lepine & Gaidos 2011) in the *K2* field of view until the end of the mission. With an increase of the sample size by a factor >3 we obtained better statis-

* Corresponding author: e-mail: raetz@astro.uni-tuebingen.de

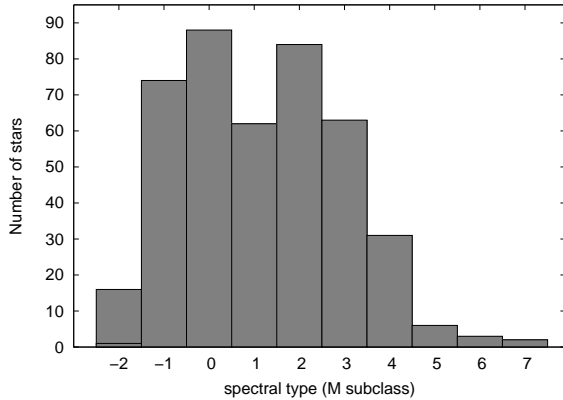


Fig. 1 Distribution of the spectral types for our *K2* M dwarf sample. The spectral types were obtained from the $V - J$ calibration given in Stelzer et al. (2016). Negative values denote spectral types earlier than M.

tics to understand the behavior around the critical rotation period of ~ 10 d.

2 The sample

Our study is based on the Superblink proper motion catalog (Lepine & Gaidos 2011), an all-sky catalog of ~ 9000 M dwarf stars with apparent infrared magnitude $J < 10$. Until the end of the mission 430 targets during 20 *K2* campaigns (C0-C19) were observed. Because of the overlap of some campaign fields we obtained in total 485 long cadence LCs.

2.1 Stellar parameters

The derivation of fundamental stellar parameters (effective temperature, mass, radius, and bolometric luminosity) was done as explained by Stelzer et al. (2016). In short, we used the empirical and semi-empirical relations of Mann et al. (2015; coefficients of the relations taken from the erratum, Mann et al. 2016) which are based on the colors $V - J$, $J - H$ and the absolute magnitude in the 2MASS K -band, M_{K_s} . Magnitudes from the UCAC4 catalog (Zacharias et al. 2013) and the AAVSO Photometric All Sky Survey (APASS; Henden & Munari 2014) were used for the calculations. To compute the M_{K_s} from the given magnitudes we used the empirical linear calibration of Stelzer et al. (2016, their Eq. 1). All stellar parameters and their uncertainties were then calculated using the following Monte Carlo approach. For each star we created 10 000 data sets of $V - J$, $J - H$ and M_{K_s} , randomly chosen from normal distributions defined by their error bars, and computed the stellar parameters. The final values were then determined as the mean and the standard deviation of the resulting distribution. The uncertainties of the relations of Mann et al. (2015) were included in the analysis. The distance was calculated from the distance modulus using the apparent magnitude in the 2MASS K -band and M_{K_s} . Because of the higher precision

of the V -band UCAC4 magnitude compared to the one provided by Lepine & Gaidos (2011), we estimated a spectral type based on the $V - J$ color using the relations given in Stelzer et al. (2016, their Eq. 2 and 3). Our full target list with the stellar parameters is given in Table A1 in the appendix¹, the distribution of the spectral types in our sample is shown in Fig. 1.

2.2 Multiplicity

Potential multiplicity of our target stars can affect our analysis in two ways. In the case of close visual binaries that are only separated by a few arcseconds the companion will contaminate the photometry of our target. On the other hand, very close eclipsing or spectroscopic binaries are well known to show strong flares and an enhanced flare frequency as shown in studies by, e.g., Mathioudakis et al. (1992), Morgan et al. (2012), or Skinner et al. (2017). Hence, knowing the multiplicity status of our stars is crucial for the interpretation of our results. Therefore, we searched all stars in our *K2* M dwarf sample for evidence of multiplicity.

One prominent example from our sample is the common proper motion pair CU Cnc (EPIC 211944670, GJ 2069A, HIP 41824) and CV Cnc (EPIC 211944856, GJ 2069B) that is actually a quintuple system. CU Cnc is a known eclipsing M dwarf binary (Delfosse et al. 1999a) with a direct imaging companion candidate (Beuzit et al. 2004) while CV Cnc is itself a visual binary (Delfosse et al. 1999b). In Raetz et al. (2020) we showed in a systematic study comparing rotation and activity in short- and long-cadence *K2* data of M dwarfs, that the highest flare rate in our sample was observed on CU Cnc. This strengthens the hypothesis that flares might be induced by the presence of a close companion.

We searched all 430 stars in the Washington Visual Double Star (WDS) Catalog (Mason et al. 2001) for information about multiplicity. In order to check for eclipsing and spectroscopic binaries we matched the General Catalogue of Variable Stars (Samus et al. 2017) and the 9th Catalogue of Spectroscopic Binary Orbits (Pourbaix et al. 2004) to our target list. To search for additional visual binaries we conducted a common proper motion analysis for all targets in our sample using the *Gaia* Data Release 2 (Gaia Collaboration et al. 2018). We downloaded all *Gaia* sources within a radius of 1 arcmin (\sim size of a *K2* target pixel file) around each of the M dwarfs. Then we compared for each of these lists the proper motions in right ascension and declination of all *Gaia* sources to the proper motion of our M dwarf target. If the proper motion of a *Gaia* source was within 10% of the proper motion of the M dwarf we considered them as a proper motion pair. We found 38 pairs in 34 systems (for four pairs both components have an individual EPIC number and both belong to our M dwarf sample) of which 26 were also listed in the WDS catalog.

¹ The tables are available in ascii format at <http://straetz.stiller-berg.de/7.html>

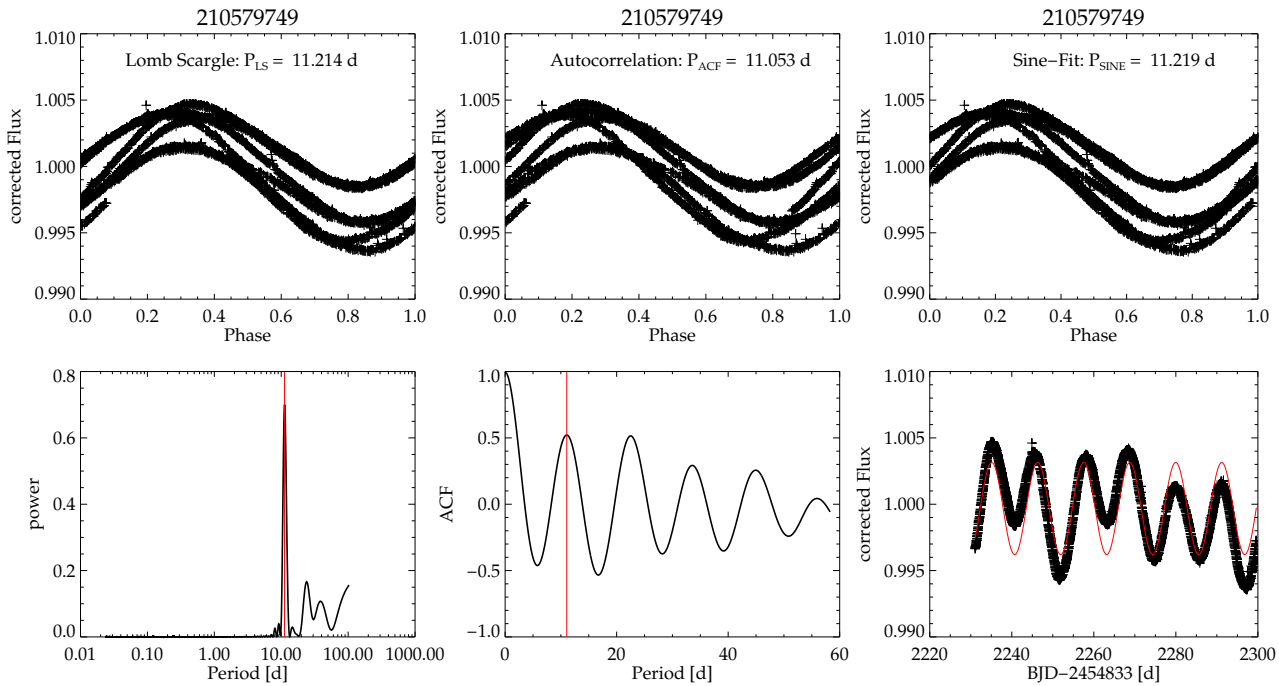


Fig. 2 Example of the three period search methods LS, ACF and sine-fitting for EPIC 210579749 observed in campaign C4. The top panels show the LCs phase-folded with the periods obtained with the different methods. The bottom panel shows the LS periodogram, the ACF and the original LC with the sine fit.

Stelzer et al. (2016) list 15 targets from our sample that show evidence for binarity which are included in our compilation. In total, we found evidence of multiplicity for 96 targets. They are all given in Table B1 in the appendix. The visual companions from the WDS catalog have separations between 0.1 and 305 arcsec. Companions with separations larger than ~ 40 arcsec (10 pixels of *K2* with an image scale of 3.98 arcsec per pixel) will not influence our analysis and are considered as single stars in the following. Consequently, 30 out of the 96 targets with evidence for multiplicity were subsequently classified as singles. The fraction of stars from the whole sample with evidences for companions is $\sim 15\%$. That is slightly higher but similar to the results of Stelzer et al. (2016, $\sim 11\%$ binarity fraction.)

3 K2 Data analysis

Vanderburg & Johnson (2014) provide fully reduced and detrended LCs for all targets from our *K2* M dwarf sample that we downloaded from the website of A. Vanderburg².

For our analysis of the rotation-activity relation we extracted the following parameters from each individual LC: (1) rotation period, (2) photometric activity indicators (stan-

² <https://www.cfa.harvard.edu/~avanderb/k2.html>

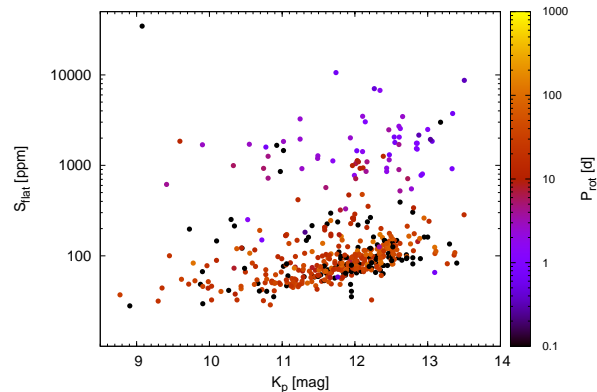


Fig. 3 Standard deviation of the flattened and cleaned LC S_{flat} over magnitude in the *Kepler* band K_p . Color-coded is the rotation period of the stars. The stars we could not detect any period are shown in black.

dard deviation of the full LC, standard deviation of the flattened and cleaned LC, amplitude of the rotational signal, flare frequency, peak flare amplitude). The definition of these properties are given in Sect. 3.2, 3.3 and 3.4. A detailed description of the determination of these properties can be found in Stelzer et al. (2016). The rotation periods and the

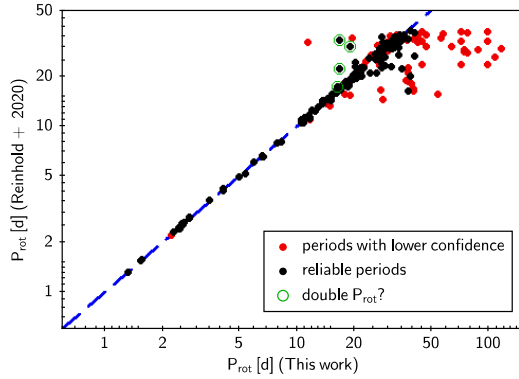


Fig. 4 Comparison between the period measurements from this work with the ones from Reinhold et al. (2020). Rotation periods of 161 stars are found in both samples. The black and red symbols denote the stars that we flagged as having reliable periods and periods with lower confidence, respectively. The green circles mark the stars where the LC is ambiguous between a period and twice its value.

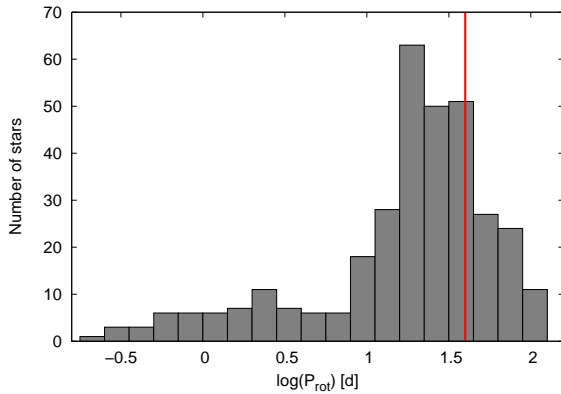


Fig. 5 Distribution of P_{rot} for the 341 M dwarfs with a measurable rotation period. The red solid line marks our defined transition between reliable periods and periods with less confidence.

values for the measured photometric activity indicators for our targets are given in Table A2 in the appendix.

3.1 Period search

The rotation period, P_{rot} , was measured with standard time series analysis techniques, a Lomb Scargle periodogram (LS; Lomb 1976 and Scargle 1982) and the autocorrelation function (ACF). Finally as a third method, we fitted the LCs with a sine function which also yields a tentative period estimate for stars that exceed the *K2* monitoring baseline of ~ 70 – 80 d. The LCs of our sample were phase-folded with the periods of all three methods. In Fig. 2 an example for the different period search methods for one of the targets from our sample is shown. A file with such figures for all 485 LCs from the 430 targets in our *K2* M dwarf sample is available

online. Among the results obtained for the three different methods, the period that best represents the LCs was selected by eye-inspection and was then used in the further analysis. Uncertainties on the rotation periods are given as the standard deviation of the period estimates from the different methods.

3.2 Activity diagnostics from rotation cycles

Because P_{rot} is derived from the periodic brightness variations that are caused by cool spots on the stellar surface, the period search yields simultaneously the amplitude of photometric variability associated with these spots. The amplitude is, hence, an indication of the stellar activity level. We determined the full amplitude R_{per} (given in %) as the mean value of all amplitudes measured for each rotation cycle as defined by McQuillan et al. (2013).

In addition to R_{per} we also determined the standard deviation of the full LC S_{ph} which includes the rotational signal and all outliers. S_{ph} was introduced by Mathur et al. (2014) as a measure of the global evolution of the variability and is, hence, an important activity indicator.

3.3 Flare identification and validation

The search for flares in the *K2* LCs was done with an iterative process which consists of three steps. Firstly, boxcar smoothing of the original LC was applied. Then the smoothed LC was subtracted from the original LC which resulted in a flat LC with the rotational signal removed. Finally, all outliers that deviated by more than 3σ were flagged and removed. These 3 steps were repeated three times with decreasing width of the boxcar. The initial width of the boxcar was selected individually based on the measured rotation period. The steps of decreasing width were chosen by testing different combinations and checking the resulting flattened LC. The iterative process results in two types of LCs: (1) a flattened LC that includes all flagged outlying points, (2) a flattened and cleaned LC with both, the rotational signal and the outliers removed.

The flattened LC was used as basis for the flare identification. From all the flagged outlying points only groups of at least two consecutive upwards outliers were selected as flare candidates. To validated these candidates as flares an additional criterion was introduced as an indication of the flare shape. We require that the ratio between the flux of the flare maximum is two times higher that the flux of the last flare point (the last consecutive outlying point) which also implies, that the maximum was not allowed to be the last flare point.

For each validated flare we determined the flare amplitude, A_{peak} , by subtracting the continuum flux level given by the flattened LC at the time of the flare peak from the corresponding flux.

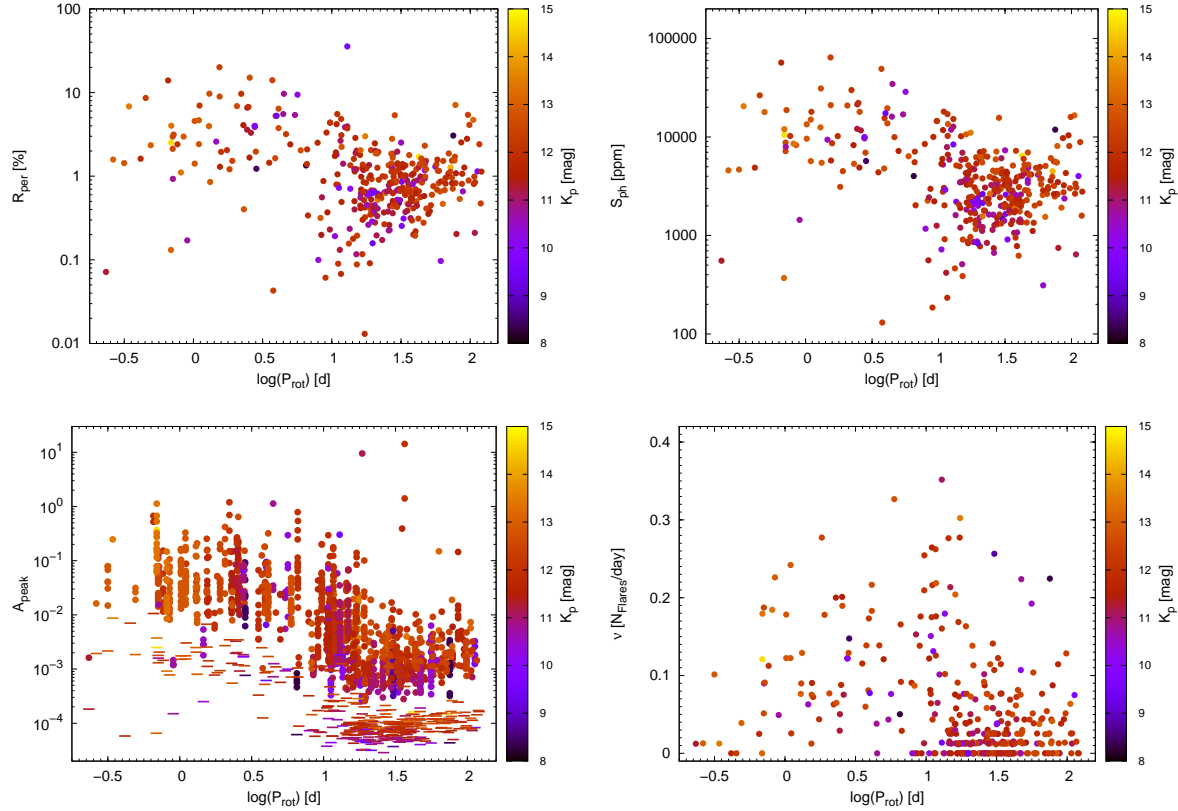


Fig. 6 Relation between rotation period and various activity indicators for all 341 targets with measurable rotation period. **Top left:** full amplitude, R_{per} , of the rotational signal given in %. **Top right:** standard deviation of the full LC, S_{ph} . **Bottom left:** flare amplitude, A_{peak} , versus rotation period for all targets that show flares. The small horizontal bars represent the standard deviation of the cleaned and flattened LCs (S_{flat}) which is a measure of our detection threshold. **Bottom right:** flare frequency, ν .

3.4 Noise level and detection bias

To investigate our flare detection bias we determined the standard deviation of the flattened and cleaned LC, S_{flat} . This value can be seen as a representation of the noise level in our data. In Fig. 3 we show the S_{flat} over the Kepler magnitude K_p . As expected the photometric noise increases towards fainter stars. In addition to the magnitude dependence of S_{flat} we see an additional scatter for a given K_p . Stelzer et al. (2016) found that fast rotators ($P_{\text{rot}} < 10$) have a higher S_{flat} than the slow rotators ($P_{\text{rot}} > 10$ d) and concluded that there is an additional underlying noise of astrophysical origin e.g. unresolved mini-flares or mini-spots for the fast rotating stars. Hence, the large scatter of S_{flat} for a given K_p is an indication that our sample comprises targets of various rotation periods. This is confirmed by the color-code in Fig. 3. The fast rotators are located well above the group of the slow rotators. With our more than three times larger sample than the one of Stelzer et al. (2016) we are able, for the first time, to distinguish two M dwarf populations in $K_p - S_{\text{flat}}$ space.

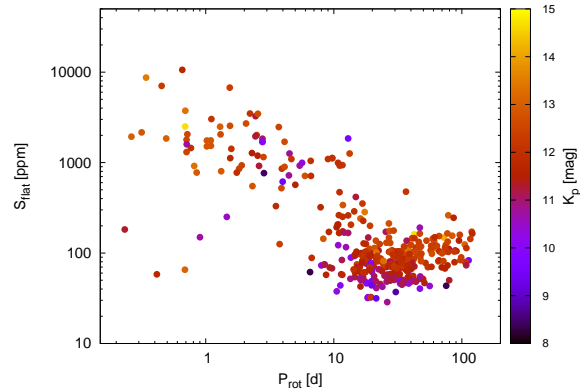


Fig. 7 Standard deviation of the flattened and cleaned LC, S_{flat} , versus rotation period for the 341 stars with measurable rotation period.

4 Results

After the eye-inspection of the phase-folded LCs resulting from the period search we sorted the targets in three different groups: those with reliable periods (flag ‘Y’ in Ta-

ble A2), periods with lower confidence (flag ‘?’) and no detected period (flag ‘N’). Since a reliable period estimate cannot be obtained with less than two full cycles we considered all periods greater than ~ 40 d (depending on the duration of the individual campaigns) as periods with lower confidence. We found 201, 140, and 89 stars to be in the groups reliable periods, periods with lower confidence, and no period, respectively. Example LCs for these three groups are shown in Fig. C1 in the appendix. For several stars all period search methods show hints of a period that is a multiple of the determined value. These stars are flagged in Table A2. For EPIC 210579749 that is shown in Fig. 2, the highest peak in the LS periodogram is ~ 4 times larger than the one of the double period. The value corresponding to our most significant period, 11d, was also found by Armstrong et al. (2016). In total, we found rotation periods for 341 stars, which is $\sim 79\%$ of all targets in our M dwarf sample. This value is in excellent agreement with the study of Stelzer et al. (2016) who already presented the rotation periods for the Lepine & Gaidos (2011) M dwarfs from campaigns C0-C4. Recently, Reinhold et al. (2020) published rotation periods for stars observed in *K2* campaigns C0-C18. We found that 161 stars from our sample have period measurements in Reinhold et al. (2020). The result of our rotation period comparison is shown in Fig. 4. For periods up to ~ 25 d our measurements are in excellent agreement. Most of the deviations in the longer period regime are stars with periods with lower confidence where we also expect to measure fractions or multiples of the true rotation periods. About 78% of our targets have $P_{\text{rot}} > 10$ d, and $\sim 10\%$ have $P_{\text{rot}} > 65$ d (see the distribution of P_{rot} in Fig. 5).

In Fig. 6 we show our measured activity diagnostics versus the rotation period. The upper panels show the full amplitude of the rotation signal, R_{per} , and the standard deviation of the full LC, S_{ph} . Both parameters show a clear trend to higher values for faster rotators. In particular we found larger spot amplitudes for stars with shorter rotation periods. This finding is in good agreement with the measurements of McQuillan et al. (2013) and Reinhold et al. (2020). The bottom panel of Fig. 6 show the parameters connected to flares for all stars with detected rotation period that show flares (272 stars). Again, we see a change of behavior at $P_{\text{rot}} \sim 10$ d. The faster rotators tend to have more flares (a higher flare rate) and the flares tend to have larger relative amplitudes. The larger spot amplitudes, the higher number of flares and the larger flare amplitudes account for the larger value of S_{ph} in the fast rotator regime.

All four plots in Fig. 6 are color-coded according to the *Kepler* magnitude to check if our results are biased because of different detection sensitivities. We found no evidence for such a bias since the bright and faint stars are evenly distributed among the fast and slow rotators.

The small horizontal bars in the rotation period - peak flare amplitude plot (bottom left plot of Fig. 6) represent the standard deviation of the cleaned and flattened LCs (S_{flat}) which is a measure of our detection threshold. Although we

Table 1 Results of the T-test for the comparison of flare parameters between single and multiple stars. $A_{\text{peak,max}}$ is the maximum peak flare amplitude, $\bar{\nu}$ is the average flare frequency evaluated for three samples: all stars, only fast and only slow rotators.

Parameter	singles	multiples	T-statistic	p-value
$A_{\text{peak,max}}$	9.5	14.3		
$\bar{\nu}$	0.051	0.074	-2.4	0.016
$\bar{\nu}_{P_{\text{rot}} < 10 \text{ d}}$	0.097	0.118	-1.2	0.251
$\bar{\nu}_{P_{\text{rot}} \geq 10 \text{ d}}$	0.040	0.051	-1.1	0.267

are not able to detect the smallest flares for the fast rotators, the difference in the upper envelope is a real effect. This upper envelope is defined by the maximum flare amplitudes $A_{\text{peak,max}}$ of the stars. We have calculated the mean of the $A_{\text{peak,max}}$ values separately for fast and slow rotators, and it is ~ 2 times higher for the fast rotators than for the slow rotators.

The flare frequency, ν , versus the rotation period is shown in the bottom right plot of Fig. 6. For many stars with rotation periods $P_{\text{rot}} > 10$ d we detected none or only one flare and, hence, ν is close to zero N_{flares}/d . In the fast rotator regime, $P_{\text{rot}} < 10$ d, we barely found LCs without any flares. With an average flare rate of $0.10 N_{\text{flares}}/d$ and $0.04 N_{\text{flares}}/d$ for the fast and slow rotators, respectively, we obtained $\nu_{P_{\text{rot}} < 10 \text{ d}} \sim 2.5 \times \nu_{P_{\text{rot}} > 10 \text{ d}}$. We determined the average flare frequency for the whole sample to be $\nu = 0.054 N_{\text{flares}}/d$. Note, that this number strongly depends on how many fast and slow rotators are included in our sample. Since our sample consists of a high number of slow rotators the average ν is biased towards a smaller value.

To examine if the multiplicity of our targets affect the flare parameters we splitted our sample of stars with measured rotation period in multiple systems and single stars. Then we computed for both groups the mean values for ν for all, only short and only long P_{rot} , and the maximum peak flare amplitude. We found that all values are higher for the multiple systems. To check if these results are significant, we ran a Student’s T-test. The results are summarized in Table 1. All p-values suggest that the mean values of ν for most of the tested groups are equal for singles and multiple systems. Only in the group of the complete sample we see a slight statistically significant difference. Hence, the multiple systems in our sample only marginally affect our results on the rotation-activity relation in terms of flare parameters. In Fig. B1 in the appendix we re-plotted the relation between rotation period and flare parameters (bottom panels of Fig. 6) with the multiple systems marked.

Finally, we examine the behavior S_{flat} with the rotation period. The result is shown in Fig. 7. As already noticed by Stelzer et al. (2016) in the more than three times smaller sample from campaigns C0-C4, we see a clear trend of higher S_{flat} values for lower P_{rot} . Since the same trend that is visible in the activity diagnostics related to the rota-

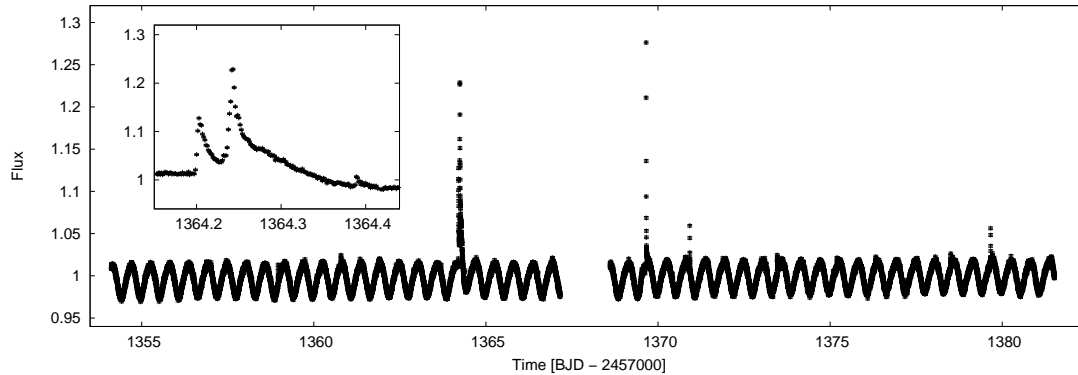


Fig. 8 Example of a Lepine & Gaidos (2011) M2 dwarf observed in *TESS* sector 2 with a clear rotation signal and a number of strong flares. The small plot shows a zoom on the first flare which consists of multiple peaks.

tion cycle and flares this might be an indication that this additional noise is caused by unresolved spot and flare activity. Hence, the underlying noise is most likely of astrophysical origin.

To summarize, we found a bimodal distribution with fast rotators showing a higher activity level than slow rotators for all examined activity diagnostics. The critical rotation period where the activity behavior changes is ~ 10 d. With a sample that is >3 times larger, we could confirm the findings by Stelzer et al. (2016). We did not find statistically significant evidence, that the multiplicity status of our targets influence our final results.

5 Outlook

Despite the outstanding capabilities of *K2*, the short observational baseline does not allow us to explore the full range of M dwarf rotation periods and the low cadence limits our study to long flares with durations of >1 h. Only 56 of the 430 targets in our *K2* M dwarf sample were observed by *K2* in short cadence mode. The comparison of the long and short cadence data are presented in detail by Raetz et al. (2020). Our study of the rotation-activity relation of M dwarfs will strongly benefit from the observation with other existing and upcoming photometric space missions i.e. *TESS* and *PLATO*.

NASA's *TESS* (Transiting Exoplanet Survey Satellite) mission is an optical space telescope dedicated for the search for planets transiting nearby stars. *TESS* was launched on April 18, 2018 and performs a near all-sky survey. The brightest $\sim 200\,000$ stars that are summarized in the Candidate Target List (CTL, Stassun et al. 2019) are observed in a 2-min cadence mode. In its two years prime mission (the mission was already extended) ~ 7000 M dwarfs from the Lepine & Gaidos (2011) catalog are observed. All of these M dwarfs are bright and will be included in the CTL. Hence, all targets will be observed with 2-min cadence. *TESS* targets during its prime mission 26 different sectors of the sky. Due to the overlap of the sectors *TESS* delivers $\sim 11\,500$ LCs in two years of operation. For about 5000 Lepine &

Gaidos (2011) M dwarfs *TESS* will provide single LCs with an observational baseline of ~ 27 d. However, $\sim 1\%$ of the targets are in the so-called continuous viewing zone where *TESS* provides thirteen 27d-light curves. Although for most of the targets only short rotation periods can be found *TESS* provides an excellent coverage for a subsample of our targets. An example of a bright ($T = 10.8$ mag) M2 dwarf observed in *TESS* sector 2 with a clear rotation signal and a number of strong flares is shown in Fig. 8. *TESS* drastically enlarges our sample of bright M dwarfs continuously monitored at high cadence and allows us to study in depth the activity and in particular the morphology of flares due to the 2-min cadence.

PLANetary Transits and Oscillations of stars (*PLATO*) is a M-class mission in ESA's Cosmic Vision programme and is foreseen to be launched in 2026. Its main goal is to find and study a large number of extrasolar planetary systems. As a photometric mission it will provide continuous high precision observations for at least 300 000 stars with a very short cadence of 25 s. This cadence will enable detailed studies of the flare shape. An example for a flare on a simulated *PLATO* LC is shown in Fig. 9. The *PLATO* fields, that are not finally decided yet, will likely include 2 long fields with an observing time of up to two years each and an additional step-and stare phase with durations of several months. If we consider the probable fields given in Barban et al. (2013), *PLATO* will observe ~ 3500 Lepine & Gaidos (2011) M dwarfs, ~ 500 of them in the two long fields. *PLATO* with its unprecedented precision, short cadence and long observational baseline, will allow us to study the magnetic activity indicators in up to now unrivaled detail.

Acknowledgements. We would especially like to thank A. Vanderburg for his public release of the analyzed *K2* light curves, upon which much of the present work is based.

References

- Armstrong, D. J., Kirk, J., Lam, K. W. F., et al. 2016, *MNRAS*, 456, 2260
- Barban, C., Goupil, M. J., Rauer, H., et al. 2013, *Fifty Years of Seismology of the Sun and Stars*, 115

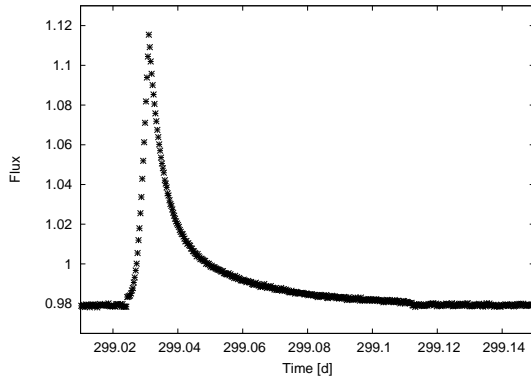


Fig. 9 Example of a flare on a simulated *PLATO* LC. The flare was constructed using the template by Davenport et al. (2014)

- Stelzer, B., Damasso, M., Scholz, A., et al. 2016, *MNRAS*, 463, 1844
 Vanderburg, A. & Johnson, J. A. 2014, *PASP*, 126, 948
 Wright, N. J., & Drake, J. J. 2016, *Nature*, 535, 526
 Wright, N. J., Newton, E. R., Williams, P. K. G., et al. 2018, *MNRAS*, 479, 2351
 Zacharias, N., Finch, C. T., Girard, T. M., et al. 2013, *AJ*, 145, 44

A M dwarf sample: stellar parameters and rotation-activity measurements

- Beuzit, J. L., Ségransan, D., Forveille, T., et al. 2004, *A&A*, 425, 997
 Bouvier, J., Matt, S. P., Mohanty, S., et al. 2014, *Protostars and Planets VI*, 433
 Davenport, J. R. A., Hawley, S. L., Hebb, L., et al. 2014, *ApJ*, 797, 122
 Delfosse, X., Forveille, T., Mayor, M., Burnet, M., & Perrier, C. 1999a, *A&A*, 341, L63
 Delfosse, X., Forveille, T., Beuzit, J.-L., et al. 1999b, *A&A*, 344, 897
 Gaia Collaboration, Brown, A. G. A., Vallenari, A., et al. 2018, *A&A*, 616, A1
 Henden, A. & Munari, U. 2014, *Contributions of the Astronomical Observatory Skalnaté Pleso*, 43, 518
 Howell, S. B., Sobek, C., Haas, M., et al. 2014, *PASP*, 126, 398
 Lépine, S., & Gaidos, E. 2011, *AJ*, 142, 138
 Lomb N. R., 1976, *Ap&SS*, 39, 447
 Mann, A. W., Feiden, G. A., Gaidos, E., Boyajian, T., & von Braun, K. 2015, *ApJ*, 804, 64
 Mann, A. W., Feiden, G. A., Gaidos, E., Boyajian, T., & von Braun, K. 2016, *ApJ*, 819, 87
 Mason, B. D., Wycoff, G. L., Hartkopf, W. I., et al. 2001, *AJ*, 122, 3466
 Mathioudakis, M., Doyle, J. G., Avgoloupis, V., Mavridis, L. N., & Seiradakis, J. H. 1992, *MNRAS*, 255, 48
 Mathur, S., Salabert, D., García, R. A., & Ceillier, T. 2014, *Journal of Space Weather and Space Climate*, 4, A15
 McQuillan, A., Aigrain, S., & Mazeh, T. 2013, *MNRAS*, 432, 1203
 Morgan, D. P., West, A. A., Garcés, A., et al. 2012, *AJ*, 144, 93
 Newton, E. R., Irwin, J., Charbonneau, D., et al. 2017, *ApJ*, 834, 85
 Pourbaix, D., Tokovinin, A. A., Batten, A. H., et al. 2004, *A&A*, 424, 727
 Raetz, S., Stelzer, B., Damasso, M., et al. 2020, *A&A*, 637, A22
 Reinhold, T., & Hekker, S. 2020, *A&A*, 635, A43
 Samus, N. N., Kazarovets, E. V., Durlevich, O. V., et al. 2017, *Astronomy Reports*, 61, 80
 Scargle J. D., 1982, *ApJ*, 263, 835
 Scholz, A. 2013, *MmSAI*, 84, 890
 Skinner, J. N., Morgan, D. P., West, A. A., Lépine, S., & Thorstensen, J. R. 2017, *AJ*, 154, 118
 Stassun, K. G., Oelkers, R. J., Paegert, M., et al. 2019, *AJ*, 158, 138

Table A1: Stellar parameters of our K2 M dwarf sample. Forty-eight targets were observed in multiple campaigns.

EPIC ID	Camp.	K_p	M_{Ks} mag	R_* [R_\odot]	M_* [M_\odot]	T_{eff} [K]	$\log L_{\text{bol}}$ [L_\odot]	d [pc]	SpT
202059183	C0	13.30	5.94 ± 0.12	0.45 ± 0.02	0.47 ± 0.02	3503 ± 84	-1.53 ± 0.05	41.0 ± 2.2	M2.5
202059188	C0	14.70	7.33 ± 0.09	0.27 ± 0.01	0.27 ± 0.01	3179 ± 81	-2.14 ± 0.04	22.1 ± 0.9	M4.5
202059190	C0	12.90	4.40 ± 0.04	0.73 ± 0.02	0.73 ± 0.01	4069 ± 81	-0.83 ± 0.02	90.7 ± 2.0	K7.0
202059192	C0	13.10	5.26 ± 0.05	0.56 ± 0.02	0.59 ± 0.01	3713 ± 81	-1.23 ± 0.03	60.1 ± 1.5	M1.0
202059193	C0	12.50	4.93 ± 0.06	0.63 ± 0.02	0.65 ± 0.02	3834 ± 82	-1.08 ± 0.03	57.1 ± 1.7	M0.0
202059195	C0	14.70	7.00 ± 0.10	0.31 ± 0.02	0.31 ± 0.01	3312 ± 82	-1.99 ± 0.04	26.0 ± 1.2	M4.0
202059197	C0	12.30	4.64 ± 0.04	0.68 ± 0.02	0.69 ± 0.01	3964 ± 81	-0.95 ± 0.02	64.1 ± 1.4	M0.0
202059198	C0	11.60	5.31 ± 0.10	0.56 ± 0.02	0.58 ± 0.02	3727 ± 99	-1.25 ± 0.04	29.3 ± 1.4	M1.0
202059199	C0	12.60	5.93 ± 0.05	0.46 ± 0.02	0.48 ± 0.01	3539 ± 84	-1.53 ± 0.03	28.8 ± 0.8	M2.5
202059203	C0	14.10	6.54 ± 0.06	0.37 ± 0.01	0.38 ± 0.01	3418 ± 80	-1.79 ± 0.03	28.5 ± 0.9	M3.0
202059204	C0	11.80	5.39 ± 0.09	0.54 ± 0.02	0.57 ± 0.02	3726 ± 94	-1.29 ± 0.04	29.6 ± 1.3	M1.5
202059207	C0	12.30	4.52 ± 0.05	0.70 ± 0.02	0.72 ± 0.02	4019 ± 82	-0.89 ± 0.02	69.4 ± 1.7	K7.0
202059208	C0	12.20	5.10 ± 0.07	0.59 ± 0.02	0.62 ± 0.02	3812 ± 83	-1.16 ± 0.03	43.8 ± 1.5	M0.5
202059210	C0	11.90	4.81 ± 0.07	0.65 ± 0.02	0.67 ± 0.02	3926 ± 84	-1.02 ± 0.03	46.4 ± 1.6	M0.0
202059215	C0	13.00	5.16 ± 0.06	0.58 ± 0.02	0.61 ± 0.02	3773 ± 82	-1.18 ± 0.03	60.8 ± 1.8	M0.5
202059221	C0	12.20	6.01 ± 0.07	0.44 ± 0.02	0.46 ± 0.01	3499 ± 86	-1.56 ± 0.03	19.2 ± 0.7	M2.5
202059222	C0	14.20	6.76 ± 0.05	0.34 ± 0.01	0.35 ± 0.01	3308 ± 79	-1.89 ± 0.02	26.3 ± 0.6	M3.5
202059223	C0	14.30	7.04 ± 0.06	0.31 ± 0.01	0.31 ± 0.01	3288 ± 80	-2.01 ± 0.03	21.2 ± 0.7	M4.0
202059224	C0	13.40	6.05 ± 0.07	0.44 ± 0.02	0.46 ± 0.01	3478 ± 81	-1.58 ± 0.03	32.8 ± 1.2	M2.5
202059229	C0	11.60	5.30 ± 0.05	0.56 ± 0.02	0.58 ± 0.01	3689 ± 82	-1.24 ± 0.03	22.9 ± 0.6	M1.0
202059231	C0	13.50	6.06 ± 0.09	0.43 ± 0.02	0.45 ± 0.02	3527 ± 83	-1.59 ± 0.04	30.4 ± 1.3	M2.5
202059243	C0	12.30	4.94 ± 0.09	0.62 ± 0.02	0.64 ± 0.02	3828 ± 86	-1.09 ± 0.04	54.0 ± 2.2	M0.5
201237257	C1	10.59	4.88 ± 0.06	0.63 ± 0.02	0.65 ± 0.02	3866 ± 87	-1.06 ± 0.03	33.9 ± 1.0	M0.0
201323410	C1	12.34	6.39 ± 0.06	0.39 ± 0.01	0.40 ± 0.01	3412 ± 80	-1.73 ± 0.03	28.8 ± 0.9	M3.0
201364753	C1	11.46	4.90 ± 0.07	0.63 ± 0.02	0.65 ± 0.02	3853 ± 87	-1.06 ± 0.03	49.4 ± 1.7	M0.0
201367065	C1	11.57	4.72 ± 0.06	0.67 ± 0.02	0.68 ± 0.02	3914 ± 87	-0.98 ± 0.03	58.7 ± 1.6	M0.0
201460770	C1	11.58	5.18 ± 0.04	0.58 ± 0.02	0.60 ± 0.01	3768 ± 82	-1.19 ± 0.02	43.8 ± 1.0	M1.0
201481218	C1	9.62	4.88 ± 0.09	0.63 ± 0.03	0.65 ± 0.02	3875 ± 89	-1.06 ± 0.04	22.3 ± 1.0	M0.0
201482319	C1	12.11	7.18 ± 0.10	0.29 ± 0.01	0.29 ± 0.01	3252 ± 91	-2.07 ± 0.04	15.3 ± 0.8	M4.0
201497866	C1	12.27	5.96 ± 0.08	0.45 ± 0.02	0.47 ± 0.02	3549 ± 87	-1.54 ± 0.04	37.6 ± 1.5	M2.5
201498184	C1	12.38	6.15 ± 0.11	0.42 ± 0.02	0.44 ± 0.02	3479 ± 84	-1.62 ± 0.05	34.6 ± 1.7	M2.5
201506253	C1	11.37	5.03 ± 0.06	0.61 ± 0.02	0.63 ± 0.02	3816 ± 85	-1.12 ± 0.03	45.0 ± 1.3	M0.5
201518346	C1	9.78	7.58 ± 0.07	0.25 ± 0.01	0.24 ± 0.01	3152 ± 80	-2.25 ± 0.03	4.1 ± 0.1	M5.0
201568682	C1	11.63	4.61 ± 0.06	0.69 ± 0.02	0.70 ± 0.02	4012 ± 86	-0.93 ± 0.03	64.1 ± 1.9	K7.0
201597919	C1	12.62	6.47 ± 0.05	0.38 ± 0.01	0.39 ± 0.01	3389 ± 80	-1.76 ± 0.03	31.4 ± 0.8	M3.0
201611969	C1	11.55	5.82 ± 0.04	0.47 ± 0.02	0.49 ± 0.01	3552 ± 81	-1.48 ± 0.02	29.8 ± 0.7	M2.0
201675315	C1	10.91	4.73 ± 0.06	0.66 ± 0.02	0.68 ± 0.02	3900 ± 84	-0.99 ± 0.03	45.2 ± 1.3	M0.0
201717312	C1	12.10	5.74 ± 0.07	0.48 ± 0.02	0.51 ± 0.02	3542 ± 83	-1.44 ± 0.03	39.8 ± 1.4	M2.0
201717791	C1	10.94	4.86 ± 0.06	0.64 ± 0.02	0.66 ± 0.02	3873 ± 90	-1.05 ± 0.03	41.1 ± 1.3	M0.0
201718613	C1	11.41	7.01 ± 0.06	0.31 ± 0.01	0.31 ± 0.01	3261 ± 89	-2.00 ± 0.03	12.7 ± 0.4	M4.0
201719115	C1	11.91	5.42 ± 0.08	0.54 ± 0.02	0.56 ± 0.02	3643 ± 85	-1.30 ± 0.04	45.4 ± 1.8	M1.5
201719818	C1	9.98	4.73 ± 0.07	0.66 ± 0.02	0.68 ± 0.02	3937 ± 87	-0.99 ± 0.03	28.3 ± 1.0	M0.0
201779048	C1	10.78	4.66 ± 0.06	0.68 ± 0.02	0.69 ± 0.02	3954 ± 86	-0.95 ± 0.03	43.9 ± 1.3	M0.0
201806997	C1	11.74	4.43 ± 0.10	0.72 ± 0.03	0.73 ± 0.02	4038 ± 92	-0.85 ± 0.04	79.8 ± 3.8	K7.0
201842163	C1	12.03	6.07 ± 0.05	0.43 ± 0.01	0.45 ± 0.01	3574 ± 82	-1.59 ± 0.02	30.4 ± 0.7	M2.5
201867138	C1	12.14	5.27 ± 0.05	0.56 ± 0.02	0.59 ± 0.01	3743 ± 81	-1.23 ± 0.03	54.5 ± 1.5	M1.0
201909533	C1	11.49	6.05 ± 0.09	0.44 ± 0.02	0.46 ± 0.02	3549 ± 88	-1.58 ± 0.04	23.3 ± 1.1	M2.5
201912552	C1	12.47	6.24 ± 0.09	0.41 ± 0.02	0.43 ± 0.02	3471 ± 85	-1.66 ± 0.04	34.1 ± 1.5	M3.0
201917390	C1	12.47	6.90 ± 0.12	0.32 ± 0.02	0.33 ± 0.02	3308 ± 82	-1.95 ± 0.05	21.8 ± 1.2	M4.0
202571062	C2	9.41	4.26 ± 0.05	0.76 ± 0.02	0.76 ± 0.02	4110 ± 84	-0.77 ± 0.02	31.8 ± 0.8	K7.0
202748218	C2	11.81	6.63 ± 0.09	0.36 ± 0.02	0.37 ± 0.01	3340 ± 83	-1.83 ± 0.04	19.8 ± 0.9	M3.5
203083752	C2	11.76	7.26 ± 0.05	0.28 ± 0.01	0.28 ± 0.01	3182 ± 79	-2.11 ± 0.03	22.3 ± 0.6	M4.5
203099398	C2	10.63	4.82 ± 0.04	0.65 ± 0.02	0.66 ± 0.01	3862 ± 84	-1.03 ± 0.02	36.6 ± 0.8	M0.0
203124214	C2	10.34	4.49 ± 0.05	0.71 ± 0.02	0.72 ± 0.02	4033 ± 90	-0.88 ± 0.03	39.8 ± 1.1	K7.0
203354308	C2	10.50	4.96 ± 1.52	0.62 ± 0.29	0.64 ± 0.21	3819 ± 918	-1.09 ± 0.62	27.8 ± 19.5	M0.5

to be continued on the next page

Table A1 continued.

EPIC ID	Camp.	K_p	M_{Ks} mag	R_* [R_\odot]	M_* [M_\odot]	T_{eff}^* [K]	$\log L_{\text{bol}}$ [L_\odot]	d [pc]	SpT
203740889	C2	12.51	6.53 ± 0.27	0.37 ± 0.04	0.38 ± 0.04	3379 ± 100	-1.79 ± 0.11	23.9 ± 2.9	M3.0
203846654	C2	9.45	4.99 ± 0.04	0.61 ± 0.02	0.64 ± 0.01	3850 ± 84	-1.11 ± 0.02	19.1 ± 0.4	M0.5
203869467	C2	10.69	4.68 ± 0.04	0.67 ± 0.02	0.69 ± 0.01	3950 ± 84	-0.97 ± 0.02	39.1 ± 0.9	M0.0
203881088	C2	12.26	5.88 ± 0.05	0.46 ± 0.02	0.48 ± 0.01	3511 ± 81	-1.51 ± 0.02	40.0 ± 0.9	M2.5
204080947	C2	12.47	5.23 ± 0.04	0.57 ± 0.02	0.59 ± 0.01	3725 ± 80	-1.21 ± 0.02	53.9 ± 1.2	M1.0
204536344	C2	9.72	4.78 ± 0.11	0.65 ± 0.03	0.67 ± 0.02	3899 ± 92	-1.01 ± 0.05	24.5 ± 1.2	M0.0
204610472	C2	12.07	5.62 ± 0.07	0.50 ± 0.02	0.53 ± 0.02	3611 ± 83	-1.39 ± 0.03	46.8 ± 1.6	M2.0
204927969	C2	11.70	7.14 ± 0.10	0.30 ± 0.01	0.30 ± 0.01	3257 ± 86	-2.05 ± 0.04	18.7 ± 0.9	M4.0
204957517	C2	12.47	7.32 ± 0.05	0.27 ± 0.01	0.27 ± 0.01	3240 ± 83	-2.13 ± 0.02	16.6 ± 0.5	M4.5
204963027	C2	11.00	5.31 ± 1.52	0.56 ± 0.27	0.58 ± 0.22	3719 ± 792	-1.25 ± 0.62	31.1 ± 21.8	M1.0
204976998	C2	10.34	4.81 ± 0.04	0.65 ± 0.02	0.67 ± 0.01	3929 ± 85	-1.02 ± 0.02	29.7 ± 0.7	M0.0
204994054	C2	11.36	4.92 ± 0.04	0.63 ± 0.02	0.65 ± 0.01	3894 ± 81	-1.07 ± 0.02	43.7 ± 1.0	M0.0
205030726	C2	11.18	5.72 ± 0.06	0.49 ± 0.02	0.51 ± 0.01	3576 ± 91	-1.43 ± 0.03	25.9 ± 0.8	M2.0
205040974	C2	11.31	5.78 ± 0.06	0.48 ± 0.02	0.50 ± 0.01	3585 ± 85	-1.46 ± 0.03	26.2 ± 0.7	M2.0
205182959	C2	12.42	5.73 ± 0.08	0.49 ± 0.02	0.51 ± 0.02	3584 ± 83	-1.44 ± 0.04	46.5 ± 1.8	M2.0
205196227	C2	11.53	4.95 ± 0.06	0.62 ± 0.02	0.64 ± 0.01	3899 ± 87	-1.09 ± 0.03	50.4 ± 1.4	M0.5
205339436	C2	12.80	6.91 ± 0.05	0.32 ± 0.01	0.33 ± 0.01	3295 ± 81	-1.95 ± 0.02	25.2 ± 0.6	M4.0
205467732	C2	12.93	7.85 ± 0.05	0.22 ± 0.01	0.22 ± 0.01	3095 ± 81	-2.36 ± 0.02	14.7 ± 0.4	M5.0
205489894	C2	12.34	5.77 ± 0.04	0.48 ± 0.02	0.50 ± 0.01	3589 ± 80	-1.45 ± 0.02	43.6 ± 1.0	M2.0
205507325	C2	12.45	6.12 ± 0.07	0.43 ± 0.02	0.45 ± 0.01	3468 ± 81	-1.61 ± 0.03	36.5 ± 1.3	M2.5
205536237	C2	9.97	5.11 ± 0.06	0.59 ± 0.02	0.62 ± 0.01	3800 ± 84	-1.16 ± 0.03	22.1 ± 0.6	M0.5
205599283	C2	11.49	4.47 ± 0.05	0.71 ± 0.02	0.72 ± 0.02	4054 ± 86	-0.87 ± 0.03	65.4 ± 1.8	K7.0
205631193	C2	11.62	5.17 ± 0.04	0.58 ± 0.02	0.61 ± 0.01	3802 ± 90	-1.19 ± 0.02	39.9 ± 0.9	M1.0
205913009	C3	12.25	7.75 ± 0.06	0.23 ± 0.01	0.23 ± 0.01	3103 ± 87	-2.32 ± 0.03	11.8 ± 0.3	M5.0
205952383	C3	11.10	4.44 ± 0.06	0.72 ± 0.02	0.73 ± 0.02	4069 ± 85	-0.85 ± 0.03	60.0 ± 1.8	K7.0
206007536	C3	10.86	4.48 ± 0.06	0.71 ± 0.02	0.72 ± 0.02	4047 ± 85	-0.87 ± 0.03	52.0 ± 1.5	K7.0
206019392	C3	8.38	7.05 ± 0.06	0.31 ± 0.01	0.31 ± 0.01	3273 ± 86	-2.01 ± 0.03	3.9 ± 0.1	M4.0
206054454	C3	12.00	5.90 ± 0.07	0.46 ± 0.02	0.48 ± 0.01	3552 ± 86	-1.51 ± 0.03	33.9 ± 1.2	M2.5
206055065	C3	10.88	4.17 ± 0.05	0.78 ± 0.02	0.77 ± 0.02	4168 ± 86	-0.73 ± 0.02	65.6 ± 1.8	K6.0
206056832	C3	11.95	4.54 ± 0.07	0.70 ± 0.02	0.71 ± 0.02	4028 ± 86	-0.90 ± 0.03	81.7 ± 2.7	K7.0
206107346	C3	9.88	4.95 ± 0.05	0.62 ± 0.02	0.64 ± 0.01	3828 ± 84	-1.09 ± 0.03	19.5 ± 0.6	M0.5
206181550	C3	12.10	5.56 ± 0.09	0.51 ± 0.02	0.54 ± 0.02	3679 ± 83	-1.36 ± 0.04	43.0 ± 1.8	M1.5
206208968	C3	10.78	6.40 ± 0.08	0.39 ± 0.02	0.40 ± 0.01	3400 ± 81	-1.73 ± 0.04	18.0 ± 0.7	M3.0
206249569	C3	12.60	6.34 ± 0.05	0.39 ± 0.01	0.41 ± 0.01	3407 ± 81	-1.71 ± 0.02	32.7 ± 0.8	M3.0
206262223	C3	12.03	6.39 ± 0.07	0.39 ± 0.01	0.40 ± 0.01	3430 ± 84	-1.73 ± 0.03	26.8 ± 0.9	M3.0
206262336	C3	12.03	7.06 ± 0.06	0.30 ± 0.01	0.31 ± 0.01	3237 ± 88	-2.02 ± 0.03	16.6 ± 0.5	M4.0
206288689	C3	11.96	6.27 ± 0.07	0.41 ± 0.02	0.42 ± 0.01	3486 ± 86	-1.68 ± 0.03	26.3 ± 0.9	M3.0
206349327	C3	12.47	5.94 ± 0.09	0.45 ± 0.02	0.47 ± 0.02	3556 ± 82	-1.53 ± 0.04	39.7 ± 1.6	M2.5
206368165	C3	12.49	5.88 ± 0.06	0.46 ± 0.02	0.48 ± 0.01	3451 ± 83	-1.50 ± 0.03	45.2 ± 1.3	M2.0
206435478	C3	11.54	4.81 ± 0.04	0.65 ± 0.02	0.67 ± 0.01	3894 ± 82	-1.03 ± 0.02	46.8 ± 1.1	M0.0
206479389	C3	12.00	5.55 ± 0.14	0.52 ± 0.03	0.54 ± 0.03	3651 ± 88	-1.36 ± 0.06	43.6 ± 2.8	M1.5
206490189	C3	12.52	6.14 ± 0.05	0.42 ± 0.01	0.44 ± 0.01	3471 ± 81	-1.62 ± 0.02	27.7 ± 0.8	M2.5
210317378	C4	12.72	6.52 ± 0.08	0.37 ± 0.01	0.38 ± 0.01	3404 ± 82	-1.78 ± 0.03	31.5 ± 1.1	M3.0
210340480	C4	11.58	5.14 ± 0.05	0.59 ± 0.02	0.61 ± 0.01	3752 ± 82	-1.17 ± 0.03	46.0 ± 1.3	M0.5
210360545	C4	12.95	7.46 ± 0.34	0.26 ± 0.04	0.26 ± 0.04	3189 ± 103	-2.19 ± 0.14	19.2 ± 3.0	M4.5
210393283	C4	12.10	5.39 ± 0.12	0.54 ± 0.03	0.57 ± 0.02	3657 ± 86	-1.29 ± 0.05	50.5 ± 2.7	M1.5
210408563	C4	11.78	5.32 ± 0.04	0.55 ± 0.02	0.58 ± 0.01	3748 ± 80	-1.26 ± 0.02	43.8 ± 1.0	M1.0
210434433	C4	12.14	6.36 ± 0.06	0.39 ± 0.01	0.41 ± 0.01	3447 ± 82	-1.71 ± 0.03	25.1 ± 0.8	M3.0
210434769	C4	10.27	4.71 ± 0.07	0.67 ± 0.02	0.68 ± 0.02	3978 ± 87	-0.98 ± 0.03	31.3 ± 1.1	M0.0
210434976	C4	12.66	7.45 ± 0.06	0.26 ± 0.01	0.26 ± 0.01	3264 ± 80	-2.19 ± 0.03	16.8 ± 0.5	M4.5
210439387	C4	12.04	5.39 ± 0.05	0.54 ± 0.02	0.57 ± 0.01	3698 ± 80	-1.29 ± 0.03	47.4 ± 1.2	M1.5
210460280	C4	11.20	5.32 ± 0.06	0.55 ± 0.02	0.58 ± 0.01	3752 ± 81	-1.26 ± 0.03	33.0 ± 1.0	M1.0
210466658	C4	10.45	4.43 ± 0.06	0.72 ± 0.02	0.73 ± 0.02	4031 ± 85	-0.85 ± 0.03	43.7 ± 1.3	K7.0
210486424	C4	12.26	6.24 ± 0.05	0.41 ± 0.01	0.43 ± 0.01	3430 ± 80	-1.66 ± 0.03	31.3 ± 0.8	M3.0
210489654	C4	12.62	7.24 ± 0.05	0.28 ± 0.01	0.28 ± 0.01	3235 ± 81	-2.10 ± 0.03	19.0 ± 0.5	M4.5
210497694	C4	12.30	5.27 ± 0.22	0.56 ± 0.04	0.59 ± 0.04	3673 ± 105	-1.23 ± 0.09	60.2 ± 6.1	M1.0
210500368	C4	11.80	5.07 ± 0.16	0.60 ± 0.03	0.62 ± 0.03	3776 ± 96	-1.14 ± 0.07	53.2 ± 3.9	M0.5

to be continued on the next page

Table A1 continued.

EPIC ID	Camp.	K_p	M_{Ks} mag	R_* [R_\odot]	M_* [M_\odot]	T_{eff}^\dagger [K]	$\log L_{\text{bol}}$ [L_\odot]	d [pc]	SpT
210500658	C4	11.40	4.13 ± 0.06	0.78 ± 0.03	0.78 ± 0.02	4142 ± 88	-0.71 ± 0.03	84.0 ± 2.5	K6.0
210502828	C4	11.15	4.57 ± 0.10	0.69 ± 0.03	0.71 ± 0.02	4012 ± 91	-0.92 ± 0.04	53.9 ± 2.5	K7.0
210535241	C4	12.02	5.00 ± 0.04	0.61 ± 0.02	0.63 ± 0.01	3846 ± 82	-1.11 ± 0.02	61.1 ± 1.3	M0.5
210579749	C4	9.98	5.53 ± 0.09	0.52 ± 0.02	0.54 ± 0.02	3643 ± 83	-1.35 ± 0.04	17.1 ± 0.7	M1.5
210580056	C4	9.30	5.01 ± 0.12	0.61 ± 0.03	0.63 ± 0.02	3817 ± 89	-1.12 ± 0.05	17.7 ± 1.0	M0.5
210585703	C4	11.61	5.26 ± 0.06	0.56 ± 0.02	0.59 ± 0.02	3670 ± 82	-1.23 ± 0.03	43.1 ± 1.3	M1.0
210592074	C4	11.44	4.37 ± 0.07	0.74 ± 0.03	0.74 ± 0.02	4090 ± 88	-0.82 ± 0.03	71.0 ± 2.5	K7.0
210613397	C4	11.99	5.38 ± 0.77	0.54 ± 0.13	0.57 ± 0.13	3728 ± 281	-1.28 ± 0.31	48.8 ± 17.3	M1.0
210693497	C4	12.14	5.78 ± 0.05	0.48 ± 0.02	0.50 ± 0.01	3584 ± 80	-1.46 ± 0.03	38.9 ± 1.0	M2.0
210707811	C4	12.81	6.82 ± 0.05	0.33 ± 0.01	0.34 ± 0.01	3325 ± 80	-1.92 ± 0.02	27.2 ± 0.6	M3.5
210757663	C4	12.10	5.11 ± 0.26	0.59 ± 0.05	0.61 ± 0.05	3768 ± 120	-1.16 ± 0.11	59.3 ± 7.3	M0.5
210778181	C4	11.15	4.74 ± 0.06	0.66 ± 0.02	0.68 ± 0.02	3904 ± 96	-0.99 ± 0.03	50.5 ± 1.4	M0.0
210941195	C4	13.36	5.92 ± 0.09	0.46 ± 0.02	0.48 ± 0.02	3541 ± 84	-1.52 ± 0.04	36.0 ± 1.6	M2.5
211006744	C4	13.27	4.91 ± 0.10	0.63 ± 0.03	0.65 ± 0.02	3837 ± 89	-1.07 ± 0.04	69.1 ± 3.3	M0.0
211008819	C4	10.10	4.87 ± 0.14	0.63 ± 0.03	0.66 ± 0.03	3904 ± 99	-1.05 ± 0.06	24.7 ± 1.6	M0.0
211029843	C4	12.71	5.65 ± 0.07	0.50 ± 0.02	0.52 ± 0.02	3563 ± 81	-1.40 ± 0.03	49.2 ± 1.7	M2.0
211036776	C4	12.80	5.85 ± 0.08	0.47 ± 0.02	0.49 ± 0.02	3534 ± 84	-1.49 ± 0.04	34.4 ± 1.3	M2.0
211107998	C4	13.02	6.10 ± 0.10	0.43 ± 0.02	0.45 ± 0.02	3529 ± 84	-1.60 ± 0.04	29.8 ± 1.4	M2.5
211111803	C4	11.97	5.15 ± 0.04	0.58 ± 0.02	0.61 ± 0.01	3797 ± 80	-1.18 ± 0.02	51.9 ± 1.2	M0.5
211183696	C4	11.56	6.49 ± 0.15	0.38 ± 0.02	0.39 ± 0.02	3421 ± 85	-1.77 ± 0.06	18.5 ± 1.2	M3.0
212270936	C6	12.16	5.24 ± 0.04	0.57 ± 0.02	0.59 ± 0.01	3762 ± 80	-1.22 ± 0.02	57.8 ± 1.3	M1.0
212276489	C6	11.89	5.11 ± 0.06	0.59 ± 0.02	0.62 ± 0.02	3773 ± 88	-1.16 ± 0.03	54.1 ± 1.6	M0.5
212280999	C6	12.46	6.22 ± 0.09	0.41 ± 0.02	0.43 ± 0.02	3394 ± 82	-1.65 ± 0.04	35.0 ± 1.5	M3.0
212285603	C6	10.67	6.85 ± 0.09	0.33 ± 0.01	0.33 ± 0.01	3290 ± 87	-1.93 ± 0.04	10.2 ± 0.5	M3.5
212318785	C6	12.56	6.20 ± 0.08	0.41 ± 0.02	0.43 ± 0.01	3502 ± 81	-1.65 ± 0.03	36.3 ± 1.3	M2.5
212323908	C6	12.58	6.56 ± 0.08	0.37 ± 0.01	0.38 ± 0.01	3374 ± 80	-1.80 ± 0.03	30.2 ± 1.1	M3.5
212329328	C6	11.30	4.07 ± 0.05	0.80 ± 0.03	0.79 ± 0.02	4253 ± 87	-0.68 ± 0.03	85.8 ± 2.5	K6.0
212422696	C6	13.00	7.47 ± 0.06	0.26 ± 0.01	0.26 ± 0.01	3150 ± 81	-2.20 ± 0.03	20.1 ± 0.6	M4.5
212557255	C6	11.18	5.30 ± 0.06	0.56 ± 0.02	0.58 ± 0.01	3731 ± 85	-1.25 ± 0.03	34.2 ± 1.1	M1.0
212647740	C6	12.34	5.66 ± 0.06	0.50 ± 0.02	0.52 ± 0.01	3613 ± 81	-1.41 ± 0.03	46.6 ± 1.4	M2.0
212663915	C6	11.93	4.46 ± 0.05	0.72 ± 0.02	0.72 ± 0.02	4052 ± 86	-0.86 ± 0.03	86.7 ± 2.5	K7.0
213817346	C7	13.34	8.26 ± 0.05	0.19 ± 0.01	0.19 ± 0.00	3034 ± 81	-2.54 ± 0.02	12.8 ± 0.3	M6.0
214089305	C7	12.52	6.05 ± 0.05	0.44 ± 0.01	0.46 ± 0.01	3495 ± 80	-1.58 ± 0.02	41.3 ± 0.9	M2.5
214269391	C7	9.35	4.74 ± 0.14	0.66 ± 0.03	0.68 ± 0.03	3901 ± 101	-0.99 ± 0.06	19.4 ± 1.3	M0.0
214787262	C7	12.53	6.54 ± 0.05	0.37 ± 0.01	0.38 ± 0.01	3382 ± 80	-1.80 ± 0.02	29.0 ± 0.7	M3.0
215004972	C7	11.32	4.57 ± 0.05	0.69 ± 0.02	0.71 ± 0.02	3984 ± 85	-0.92 ± 0.03	54.6 ± 1.5	K7.0
215632123	C7	8.45	6.97 ± 0.05	0.31 ± 0.01	0.32 ± 0.01	3276 ± 81	-1.98 ± 0.02	4.8 ± 0.1	M4.0
215818496	C7	11.02	6.40 ± 0.05	0.39 ± 0.01	0.40 ± 0.01	3370 ± 83	-1.73 ± 0.03	16.1 ± 0.4	M3.0
215969058	C7	11.58	5.59 ± 0.07	0.51 ± 0.02	0.53 ± 0.02	3623 ± 92	-1.38 ± 0.03	37.2 ± 1.3	M1.5
216273315	C7	12.39	5.43 ± 0.04	0.54 ± 0.02	0.56 ± 0.01	3656 ± 86	-1.30 ± 0.02	43.2 ± 1.0	M1.5
216848322	C7	11.98	5.18 ± 0.05	0.58 ± 0.02	0.60 ± 0.01	3766 ± 81	-1.19 ± 0.03	56.7 ± 1.6	M1.0
216892056	C7	12.50	5.92 ± 0.04	0.46 ± 0.01	0.48 ± 0.01	3525 ± 80	-1.52 ± 0.02	43.8 ± 0.9	M2.5
218121888	C7	12.04	7.32 ± 0.05	0.27 ± 0.01	0.27 ± 0.01	3184 ± 79	-2.13 ± 0.02	22.6 ± 0.5	M4.5
218790299	C7	10.72	4.50 ± 0.08	0.71 ± 0.03	0.72 ± 0.02	4081 ± 95	-0.88 ± 0.04	43.5 ± 1.7	K7.0
219448194	C7	12.04	5.44 ± 0.04	0.53 ± 0.02	0.56 ± 0.01	3696 ± 82	-1.31 ± 0.02	48.1 ± 1.1	M1.5
220209255	C8	11.73	4.32 ± 0.06	0.74 ± 0.02	0.75 ± 0.02	4168 ± 86	-0.80 ± 0.03	83.5 ± 2.5	K7.0
220215093	C8	12.35	7.37 ± 0.08	0.27 ± 0.01	0.27 ± 0.01	3329 ± 84	-2.15 ± 0.04	15.4 ± 0.6	M4.5
220237354	C8	12.22	5.51 ± 0.12	0.52 ± 0.02	0.55 ± 0.02	3693 ± 86	-1.34 ± 0.05	47.5 ± 2.6	M1.5
220256064	C8	11.95	4.45 ± 0.13	0.72 ± 0.03	0.73 ± 0.02	4072 ± 100	-0.86 ± 0.05	84.0 ± 5.1	K7.0
220265960	C8	12.78	7.20 ± 0.19	0.29 ± 0.02	0.29 ± 0.02	3252 ± 89	-2.08 ± 0.08	20.6 ± 1.8	M4.0
220266256	C8	11.85	4.66 ± 0.09	0.68 ± 0.03	0.69 ± 0.02	3956 ± 87	-0.95 ± 0.04	70.7 ± 2.9	M0.0
220287795	C8	12.05	5.07 ± 0.06	0.60 ± 0.02	0.62 ± 0.01	3806 ± 84	-1.14 ± 0.03	59.1 ± 1.6	M0.5
220308656	C8	12.54	6.08 ± 0.13	0.43 ± 0.02	0.45 ± 0.02	3465 ± 86	-1.59 ± 0.05	38.6 ± 2.3	M2.5
220323325	C8	11.48	5.21 ± 0.07	0.57 ± 0.02	0.60 ± 0.02	3755 ± 87	-1.21 ± 0.03	41.2 ± 1.4	M1.0
220350328	C8	11.13	4.31 ± 0.07	0.75 ± 0.03	0.75 ± 0.02	4093 ± 88	-0.80 ± 0.03	67.8 ± 2.4	K7.0
220412416	C8	11.88	4.73 ± 0.07	0.66 ± 0.02	0.68 ± 0.02	3936 ± 85	-0.99 ± 0.03	69.6 ± 2.3	M0.0
220460555	C8	11.63	4.03 ± 0.06	0.81 ± 0.03	0.79 ± 0.02	4247 ± 87	-0.66 ± 0.03	100.4 ± 2.9	K6.0

to be continued on the next page

Table A1 continued.

EPIC ID	Camp.	K_p	M_{Ks} mag	R_* [R_\odot]	M_* [M_\odot]	T_{eff}^* [K]	$\log L_{\text{bol}}$ [L_\odot]	d [pc]	SpT
220467322	C8	11.05	4.76 ± 0.09	0.66 ± 0.03	0.67 ± 0.02	3942 ± 92	-1.00 ± 0.04	44.7 ± 2.0	M0.0
220475592	C8	11.95	5.81 ± 0.09	0.47 ± 0.02	0.50 ± 0.02	3548 ± 90	-1.47 ± 0.04	35.7 ± 1.6	M2.0
220501313	C8	11.14	4.87 ± 0.04	0.64 ± 0.02	0.66 ± 0.01	3866 ± 82	-1.05 ± 0.02	44.4 ± 1.0	M0.0
220581451	C8	13.06	7.61 ± 0.05	0.25 ± 0.01	0.24 ± 0.01	3174 ± 80	-2.26 ± 0.02	18.1 ± 0.4	M5.0
220604532	C8	12.74	7.54 ± 0.07	0.25 ± 0.01	0.25 ± 0.01	3150 ± 83	-2.23 ± 0.03	16.5 ± 0.6	M4.5
220611593	C8	12.16	4.72 ± 0.08	0.66 ± 0.02	0.68 ± 0.02	3940 ± 87	-0.98 ± 0.04	77.7 ± 3.0	M0.0
220623047	C8	12.09	5.44 ± 0.06	0.53 ± 0.02	0.56 ± 0.01	3628 ± 85	-1.31 ± 0.03	48.1 ± 1.4	M1.5
220624740	C8	11.68	5.94 ± 0.05	0.45 ± 0.01	0.47 ± 0.01	3541 ± 81	-1.53 ± 0.02	27.2 ± 0.6	M2.5
220676900	C8	11.63	5.43 ± 0.20	0.54 ± 0.04	0.56 ± 0.04	3689 ± 105	-1.31 ± 0.08	38.9 ± 3.7	M1.5
220677352	C8	11.28	5.35 ± 0.18	0.55 ± 0.03	0.57 ± 0.03	3701 ± 99	-1.27 ± 0.07	34.8 ± 2.9	M1.0
220677738	C8	12.18	5.84 ± 0.06	0.47 ± 0.02	0.49 ± 0.01	3630 ± 84	-1.49 ± 0.03	38.0 ± 1.1	M2.0
220706618	C8	11.94	5.83 ± 0.05	0.47 ± 0.02	0.49 ± 0.01	3595 ± 82	-1.48 ± 0.03	34.0 ± 0.9	M2.0
220732658	C8	11.88	5.14 ± 0.65	0.59 ± 0.12	0.61 ± 0.11	3781 ± 255	-1.17 ± 0.26	54.3 ± 16.2	M0.5
201077482	C10	11.22	5.09 ± 0.06	0.59 ± 0.02	0.62 ± 0.02	3774 ± 82	-1.15 ± 0.03	39.6 ± 1.2	M0.5
201128047	C10	12.38	5.40 ± 0.05	0.54 ± 0.02	0.57 ± 0.01	3691 ± 82	-1.29 ± 0.03	53.8 ± 1.4	M1.5
201223580	C10	12.23	5.46 ± 0.07	0.53 ± 0.02	0.55 ± 0.02	3718 ± 83	-1.32 ± 0.03	49.2 ± 1.7	M1.5
201288384	C10	10.75	4.65 ± 0.06	0.68 ± 0.02	0.69 ± 0.02	3985 ± 85	-0.95 ± 0.03	43.3 ± 1.3	M0.0
201296234	C10	12.07	4.74 ± 0.11	0.66 ± 0.03	0.68 ± 0.02	3920 ± 91	-0.99 ± 0.05	75.6 ± 3.8	M0.0
201416151	C10	10.62	4.62 ± 0.07	0.68 ± 0.02	0.70 ± 0.02	3938 ± 97	-0.94 ± 0.03	40.4 ± 1.4	M0.0
201431768	C10	10.62	4.88 ± 0.04	0.63 ± 0.02	0.65 ± 0.01	3829 ± 86	-1.06 ± 0.02	34.8 ± 0.8	M0.0
201506654	C10	12.11	8.47 ± 0.07	0.18 ± 0.01	0.17 ± 0.00	3012 ± 87	-2.63 ± 0.03	6.5 ± 0.2	M6.0
201530621	C10	12.39	5.91 ± 0.19	0.46 ± 0.03	0.48 ± 0.03	3501 ± 93	-1.52 ± 0.08	41.4 ± 3.7	M2.5
201659529	C10	12.13	6.57 ± 0.05	0.36 ± 0.01	0.38 ± 0.01	3355 ± 80	-1.81 ± 0.03	23.5 ± 0.6	M3.5
228711280	C10	12.76	6.62 ± 0.21	0.36 ± 0.03	0.37 ± 0.03	3375 ± 91	-1.83 ± 0.08	30.5 ± 2.9	M3.5
228726301	C10	12.86	6.78 ± 0.08	0.34 ± 0.01	0.34 ± 0.01	3300 ± 82	-1.90 ± 0.03	29.5 ± 1.1	M3.5
228750455	C10	11.93	4.54 ± 0.09	0.70 ± 0.03	0.71 ± 0.02	4026 ± 92	-0.90 ± 0.04	79.2 ± 3.5	K7.0
228757142	C10	11.08	5.37 ± 0.06	0.55 ± 0.02	0.57 ± 0.01	3688 ± 83	-1.28 ± 0.03	33.4 ± 1.0	M1.0
228782343	C10	11.68	4.34 ± 0.05	0.74 ± 0.02	0.74 ± 0.02	4108 ± 82	-0.81 ± 0.02	82.7 ± 2.1	K7.0
228808502	C10	12.51	6.87 ± 0.10	0.33 ± 0.02	0.33 ± 0.02	3305 ± 82	-1.94 ± 0.04	23.3 ± 1.1	M3.5
228857363	C10	11.68	6.26 ± 0.06	0.41 ± 0.01	0.42 ± 0.01	3388 ± 81	-1.67 ± 0.03	31.7 ± 0.9	M3.0
228858734	C10	12.35	6.97 ± 0.05	0.31 ± 0.01	0.32 ± 0.01	3278 ± 81	-1.98 ± 0.03	19.8 ± 0.5	M4.0
228861595	C10	11.80	4.96 ± 0.06	0.62 ± 0.02	0.64 ± 0.02	3816 ± 82	-1.09 ± 0.03	57.2 ± 1.7	M0.5
228864582	C10	12.88	7.34 ± 0.16	0.27 ± 0.02	0.27 ± 0.02	3197 ± 85	-2.14 ± 0.07	19.8 ± 1.5	M4.5
228885036	C10	10.74	4.66 ± 0.06	0.68 ± 0.02	0.69 ± 0.02	3955 ± 84	-0.96 ± 0.03	43.2 ± 1.4	M0.0
228901441	C10	11.64	6.76 ± 0.08	0.34 ± 0.01	0.35 ± 0.01	3369 ± 84	-1.89 ± 0.04	16.5 ± 0.7	M3.5
228972691	C10	12.40	6.83 ± 0.06	0.33 ± 0.01	0.34 ± 0.01	3376 ± 83	-1.92 ± 0.03	21.7 ± 0.7	M3.5
228982481	C10	11.78	4.66 ± 0.09	0.68 ± 0.03	0.69 ± 0.02	3935 ± 89	-0.96 ± 0.04	70.3 ± 3.2	M0.0
228992431	C10	12.45	5.58 ± 0.07	0.51 ± 0.02	0.53 ± 0.02	3637 ± 82	-1.37 ± 0.03	51.1 ± 1.8	M1.5
229043460	C10	12.12	5.34 ± 0.07	0.55 ± 0.02	0.57 ± 0.02	3705 ± 85	-1.27 ± 0.03	50.0 ± 1.7	M1.0
229081889	C10	12.22	5.52 ± 0.07	0.52 ± 0.02	0.54 ± 0.02	3631 ± 88	-1.35 ± 0.03	48.4 ± 1.7	M1.5
229122988	C10	12.30	5.43 ± 0.06	0.54 ± 0.02	0.56 ± 0.01	3664 ± 84	-1.31 ± 0.03	50.1 ± 1.5	M1.5
229149393	C10	11.41	4.55 ± 0.09	0.70 ± 0.03	0.71 ± 0.02	4006 ± 92	-0.91 ± 0.04	63.4 ± 2.8	K7.0
223636719	C11	10.56	4.89 ± 0.04	0.63 ± 0.02	0.65 ± 0.01	3854 ± 84	-1.06 ± 0.02	33.2 ± 0.7	M0.0
224945540	C11	13.37	6.15 ± 0.05	0.42 ± 0.01	0.44 ± 0.01	3453 ± 81	-1.62 ± 0.02	40.2 ± 1.0	M2.5
225420708	C11	10.30	5.03 ± 1.52	0.60 ± 0.29	0.63 ± 0.22	3840 ± 841	-1.13 ± 0.62	26.6 ± 18.7	M0.5
226240066	C11	12.54	6.48 ± 0.05	0.38 ± 0.01	0.39 ± 0.01	3379 ± 80	-1.77 ± 0.03	31.5 ± 0.8	M3.0
229432919	C11	11.05	4.58 ± 0.06	0.69 ± 0.02	0.70 ± 0.02	3940 ± 92	-0.92 ± 0.03	52.5 ± 1.6	K7.0
230510723	C11	11.79	5.54 ± 0.05	0.52 ± 0.02	0.54 ± 0.01	3619 ± 82	-1.35 ± 0.03	39.2 ± 1.0	M1.5
230751558	C11	12.65	6.04 ± 0.06	0.44 ± 0.02	0.46 ± 0.01	3478 ± 80	-1.57 ± 0.03	31.8 ± 1.0	M2.5
231116934	C11	12.00	5.27 ± 0.05	0.56 ± 0.02	0.59 ± 0.01	3748 ± 82	-1.23 ± 0.03	51.4 ± 1.3	M1.0
231179480	C11	10.48	4.75 ± 0.07	0.66 ± 0.02	0.68 ± 0.02	3924 ± 88	-1.00 ± 0.03	35.3 ± 1.3	M0.0
231875643	C11	12.38	6.85 ± 0.05	0.33 ± 0.01	0.33 ± 0.01	3322 ± 81	-1.93 ± 0.02	22.4 ± 0.5	M3.5
232017621	C11	13.18	7.45 ± 0.05	0.26 ± 0.01	0.26 ± 0.01	3209 ± 80	-2.19 ± 0.02	20.8 ± 0.5	M4.5
232097582	C11	11.15	6.18 ± 0.21	0.42 ± 0.03	0.43 ± 0.03	3486 ± 98	-1.64 ± 0.08	23.3 ± 2.2	M2.5
233488533	C11	12.95	7.29 ± 0.05	0.28 ± 0.01	0.28 ± 0.01	3233 ± 81	-2.12 ± 0.02	21.2 ± 0.6	M4.5
234562190	C11	9.60	5.25 ± 0.07	0.57 ± 0.02	0.59 ± 0.02	3745 ± 98	-1.23 ± 0.03	17.7 ± 0.8	M1.0
234698848	C11	11.46	3.30 ± 0.13	0.97 ± 0.04	0.89 ± 0.02	4752 ± 140	-0.32 ± 0.05	150.6 ± 9.0	K5.0

to be continued on the next page

Table A1 continued.

EPIC ID	Camp.	K_p	M_{Ks} mag	R_* [R_\odot]	M_* [M_\odot]	T_{eff} [K]	$\log L_{\text{bol}}$ [L_\odot]	d [pc]	SpT
235067510	C11	12.12	6.11 ± 0.13	0.43 ± 0.02	0.45 ± 0.02	3465 ± 86	-1.61 ± 0.05	32.5 ± 2.0	M2.5
235070897	C11	11.06	4.55 ± 0.06	0.70 ± 0.02	0.71 ± 0.02	3949 ± 88	-0.90 ± 0.03	53.0 ± 1.6	K7.0
236285338	C11	12.35	6.50 ± 0.06	0.37 ± 0.01	0.38 ± 0.01	3392 ± 82	-1.78 ± 0.03	27.0 ± 0.8	M3.0
236305079	C11	11.33	5.22 ± 0.06	0.57 ± 0.02	0.60 ± 0.01	3776 ± 84	-1.21 ± 0.03	34.6 ± 0.9	M1.0
236469315	C11	11.41	5.67 ± 0.15	0.50 ± 0.03	0.52 ± 0.03	3536 ± 100	-1.41 ± 0.06	29.8 ± 2.1	M2.0
237853022	C11	11.09	4.14 ± 0.05	0.78 ± 0.03	0.78 ± 0.02	4186 ± 91	-0.71 ± 0.03	71.5 ± 1.9	K6.0
240451481	C11	9.73	4.50 ± 0.04	0.71 ± 0.02	0.72 ± 0.01	4026 ± 83	-0.88 ± 0.02	28.6 ± 0.6	K7.0
242219524	C11	10.72	4.92 ± 0.04	0.63 ± 0.02	0.65 ± 0.01	3864 ± 82	-1.08 ± 0.02	29.4 ± 0.7	M0.0
245919787	C12	10.33	5.36 ± 0.04	0.55 ± 0.02	0.57 ± 0.01	3733 ± 84	-1.27 ± 0.02	17.4 ± 0.4	M1.0
245983914	C12	11.97	4.97 ± 0.04	0.62 ± 0.02	0.64 ± 0.01	3807 ± 82	-1.10 ± 0.02	62.8 ± 1.4	M0.5
246043232	C12	11.67	6.13 ± 0.32	0.43 ± 0.05	0.44 ± 0.05	3502 ± 113	-1.61 ± 0.13	32.1 ± 4.7	M2.5
246048874	C12	11.97	5.13 ± 0.09	0.59 ± 0.02	0.61 ± 0.02	3761 ± 86	-1.17 ± 0.04	60.2 ± 2.5	M0.5
246069579	C12	11.19	4.61 ± 0.06	0.69 ± 0.02	0.70 ± 0.02	3964 ± 83	-0.93 ± 0.03	54.7 ± 1.5	K7.0
246159774	C12	12.10	5.27 ± 0.04	0.56 ± 0.02	0.59 ± 0.01	3696 ± 80	-1.23 ± 0.02	54.6 ± 1.2	M1.0
246175846	C12	11.21	5.26 ± 0.04	0.56 ± 0.02	0.59 ± 0.01	3749 ± 87	-1.23 ± 0.02	34.7 ± 0.8	M1.0
246215873	C12	12.00	5.25 ± 0.04	0.57 ± 0.02	0.59 ± 0.01	3713 ± 80	-1.23 ± 0.02	51.8 ± 1.2	M1.0
246226675	C12	11.92	6.82 ± 0.08	0.33 ± 0.01	0.34 ± 0.01	3330 ± 83	-1.91 ± 0.03	24.7 ± 0.9	M3.5
246253313	C12	12.82	6.29 ± 0.12	0.40 ± 0.02	0.42 ± 0.02	3477 ± 83	-1.69 ± 0.05	33.9 ± 1.8	M3.0
246338131	C12	12.25	5.08 ± 0.04	0.60 ± 0.02	0.62 ± 0.01	3819 ± 80	-1.15 ± 0.02	62.0 ± 1.4	M0.5
210491860	C13	11.60	5.12 ± 0.04	0.59 ± 0.02	0.61 ± 0.01	3754 ± 82	-1.16 ± 0.02	47.1 ± 1.0	M0.5
210596446	C13	12.00	5.56 ± 0.09	0.51 ± 0.02	0.54 ± 0.02	3633 ± 84	-1.36 ± 0.04	41.5 ± 1.7	M1.5
210651981	C4,C13	11.25	5.92 ± 0.07	0.46 ± 0.02	0.48 ± 0.02	3549 ± 83	-1.52 ± 0.03	22.8 ± 0.8	M2.5
210653579	C13	11.23	4.81 ± 0.07	0.65 ± 0.02	0.67 ± 0.02	3914 ± 84	-1.03 ± 0.03	48.1 ± 1.7	M0.0
210721261	C13	12.35	6.24 ± 0.09	0.41 ± 0.02	0.42 ± 0.02	3467 ± 81	-1.66 ± 0.04	30.8 ± 1.3	M3.0
210741091	C4,C13	11.98	5.31 ± 0.05	0.56 ± 0.02	0.58 ± 0.01	3716 ± 80	-1.25 ± 0.03	47.7 ± 1.2	M1.0
210840804	C13	12.91	6.65 ± 0.12	0.35 ± 0.02	0.36 ± 0.02	3424 ± 83	-1.84 ± 0.05	30.4 ± 1.7	M3.5
210889984	C13	11.11	4.29 ± 0.07	0.75 ± 0.03	0.75 ± 0.02	4132 ± 87	-0.79 ± 0.03	53.5 ± 1.9	K7.0
210895913	C13	12.30	6.58 ± 0.09	0.36 ± 0.02	0.37 ± 0.02	3413 ± 85	-1.81 ± 0.04	21.2 ± 0.9	M3.5
210915518	C13	12.54	5.80 ± 0.09	0.47 ± 0.02	0.50 ± 0.02	3588 ± 82	-1.47 ± 0.04	37.3 ± 1.5	M2.0
246625561	C13	12.11	6.22 ± 0.15	0.41 ± 0.02	0.43 ± 0.02	3526 ± 89	-1.65 ± 0.06	27.7 ± 1.9	M3.0
246732310	C13	11.05	4.92 ± 0.09	0.63 ± 0.02	0.65 ± 0.02	3858 ± 89	-1.08 ± 0.04	40.6 ± 1.8	M0.0
246774176	C13	11.49	6.26 ± 0.05	0.41 ± 0.01	0.42 ± 0.01	3395 ± 83	-1.67 ± 0.02	21.9 ± 0.5	M3.0
246806983	C13	11.27	5.27 ± 0.19	0.56 ± 0.04	0.59 ± 0.03	3773 ± 99	-1.23 ± 0.08	36.8 ± 3.2	M1.0
246807434	C13	12.17	6.30 ± 0.05	0.40 ± 0.01	0.42 ± 0.01	3397 ± 80	-1.69 ± 0.02	29.1 ± 0.7	M3.0
246812637	C13	12.41	6.06 ± 0.07	0.44 ± 0.02	0.45 ± 0.01	3461 ± 81	-1.58 ± 0.03	37.6 ± 1.3	M2.5
246818597	C13	8.29	6.57 ± 0.27	0.36 ± 0.04	0.37 ± 0.04	3330 ± 188	-1.81 ± 0.11	3.4 ± 0.4	M3.5
246849411	C13	11.41	4.95 ± 0.06	0.62 ± 0.02	0.64 ± 0.02	3871 ± 82	-1.09 ± 0.03	44.4 ± 1.4	M0.5
246862801	C13	11.70	5.13 ± 0.05	0.59 ± 0.02	0.61 ± 0.01	3794 ± 755	-1.17 ± 0.03	48.3 ± 1.2	M0.5
246931087	C13	10.44	4.91 ± 0.07	0.63 ± 0.02	0.65 ± 0.02	3843 ± 88	-1.07 ± 0.03	31.1 ± 1.0	M0.0
247003390	C13	11.81	4.51 ± 0.04	0.70 ± 0.02	0.72 ± 0.01	4034 ± 81	-0.89 ± 0.02	76.1 ± 1.7	K7.0
247080522	C13	12.53	6.64 ± 0.05	0.35 ± 0.01	0.36 ± 0.01	3333 ± 80	-1.84 ± 0.03	27.4 ± 0.7	M3.5
247094343	C13	12.39	5.97 ± 0.05	0.45 ± 0.01	0.47 ± 0.01	3529 ± 80	-1.54 ± 0.02	39.3 ± 0.9	M2.5
247122957	C13	12.62	6.34 ± 0.05	0.39 ± 0.01	0.41 ± 0.01	3444 ± 81	-1.71 ± 0.03	32.7 ± 0.9	M3.0
247130198	C13	9.08	5.95 ± 0.07	0.45 ± 0.02	0.47 ± 0.01	3546 ± 83	-1.53 ± 0.03	8.6 ± 0.3	M2.5
247164626	C13	12.62	6.08 ± 0.07	0.43 ± 0.02	0.45 ± 0.01	3478 ± 81	-1.59 ± 0.03	40.6 ± 1.5	M2.5
247191714	C13	11.78	5.14 ± 0.04	0.59 ± 0.02	0.61 ± 0.01	3750 ± 82	-1.17 ± 0.02	51.3 ± 1.1	M0.5
247238215	C13	11.17	5.48 ± 0.06	0.53 ± 0.02	0.55 ± 0.01	3665 ± 82	-1.33 ± 0.03	30.6 ± 0.8	M1.5
247269565	C13	11.22	5.97 ± 0.06	0.45 ± 0.02	0.47 ± 0.01	3491 ± 87	-1.55 ± 0.03	23.4 ± 0.7	M2.5
247282522	C13	10.53	4.32 ± 0.05	0.74 ± 0.02	0.75 ± 0.02	4101 ± 84	-0.80 ± 0.03	52.3 ± 1.4	K7.0
247289039	C13	12.73	6.47 ± 0.09	0.38 ± 0.02	0.39 ± 0.02	3417 ± 81	-1.76 ± 0.04	25.6 ± 1.1	M3.0
247309641	C13	13.50	7.93 ± 0.13	0.22 ± 0.01	0.21 ± 0.01	3094 ± 84	-2.40 ± 0.05	13.0 ± 0.8	M5.5
247325547	C13	11.48	5.53 ± 0.08	0.52 ± 0.02	0.54 ± 0.02	3674 ± 84	-1.35 ± 0.04	27.0 ± 1.0	M1.5
247449449	C13	12.36	6.55 ± 0.14	0.37 ± 0.02	0.38 ± 0.02	3418 ± 86	-1.80 ± 0.06	26.5 ± 1.7	M3.5
247476655	C13	11.78	4.98 ± 0.07	0.61 ± 0.02	0.64 ± 0.02	3862 ± 83	-1.10 ± 0.03	55.2 ± 1.9	M0.5
247514292	C13	12.05	4.80 ± 0.04	0.65 ± 0.02	0.67 ± 0.01	3918 ± 82	-1.02 ± 0.02	72.5 ± 1.6	M0.0
247592661	C13	11.94	6.29 ± 0.05	0.40 ± 0.01	0.42 ± 0.01	3488 ± 81	-1.68 ± 0.02	26.2 ± 0.6	M3.0
247640857	C13	11.45	4.88 ± 0.06	0.63 ± 0.02	0.65 ± 0.02	3862 ± 93	-1.06 ± 0.03	52.1 ± 1.6	M0.0

to be continued on the next page

Table A1 continued.

EPIC ID	Camp.	K_p	M_{Ks} mag	R_* [R_\odot]	M_* [M_\odot]	T_{eff}^\dagger [K]	$\log L_{\text{bol}}$ [L_\odot]	d [pc]	SpT
247657761	C13	11.35	4.64 ± 0.04	0.68 ± 0.02	0.70 ± 0.01	3939 ± 84	-0.95 ± 0.02	59.0 ± 1.3	M0.0
247679710	C13	12.34	5.43 ± 0.10	0.54 ± 0.02	0.56 ± 0.02	3665 ± 86	-1.31 ± 0.04	48.4 ± 2.3	M1.5
247725508	C13	11.97	4.89 ± 0.05	0.63 ± 0.02	0.65 ± 0.01	3896 ± 81	-1.06 ± 0.03	65.8 ± 1.7	M0.0
247730793	C13	11.17	4.74 ± 0.06	0.66 ± 0.02	0.68 ± 0.02	3894 ± 100	-0.99 ± 0.03	48.4 ± 1.4	M0.0
247734588	C13	13.11	6.88 ± 0.09	0.32 ± 0.01	0.33 ± 0.01	3302 ± 81	-1.94 ± 0.04	26.8 ± 1.1	M4.0
247744104	C13	11.51	5.10 ± 0.07	0.59 ± 0.02	0.62 ± 0.02	3786 ± 83	-1.16 ± 0.03	46.0 ± 1.6	M0.5
247827225	C13	12.36	5.40 ± 0.10	0.54 ± 0.02	0.57 ± 0.02	3679 ± 84	-1.29 ± 0.04	54.9 ± 2.6	M1.5
247867687	C13	10.77	5.80 ± 0.08	0.48 ± 0.02	0.50 ± 0.02	3552 ± 84	-1.47 ± 0.04	19.1 ± 0.7	M2.0
247905449	C13	11.88	5.28 ± 0.06	0.56 ± 0.02	0.59 ± 0.02	3736 ± 83	-1.24 ± 0.03	44.4 ± 1.3	M1.0
247909274	C13	12.52	6.74 ± 0.05	0.34 ± 0.01	0.35 ± 0.01	3321 ± 79	-1.88 ± 0.02	25.9 ± 0.6	M3.5
247969864	C13	11.15	4.44 ± 0.04	0.72 ± 0.02	0.73 ± 0.01	4026 ± 81	-0.85 ± 0.02	61.2 ± 1.3	K7.0
247983269	C13	12.58	6.10 ± 0.05	0.43 ± 0.01	0.45 ± 0.01	3540 ± 80	-1.60 ± 0.02	39.1 ± 0.9	M2.5
247988033	C13	12.08	4.82 ± 0.06	0.65 ± 0.02	0.66 ± 0.02	3891 ± 83	-1.03 ± 0.03	72.6 ± 2.2	M0.0
248030935	C13	10.38	4.89 ± 0.05	0.63 ± 0.02	0.65 ± 0.01	3844 ± 81	-1.06 ± 0.03	30.2 ± 0.8	M0.0
248042336	C13	11.81	6.16 ± 0.05	0.42 ± 0.01	0.44 ± 0.01	3435 ± 83	-1.63 ± 0.02	26.9 ± 0.7	M2.5
201497396	C14	10.10	4.43 ± 0.04	0.72 ± 0.02	0.73 ± 0.01	4032 ± 85	-0.85 ± 0.02	38.2 ± 0.8	K7.0
201501470	C14	12.61	7.37 ± 0.06	0.27 ± 0.01	0.27 ± 0.01	3231 ± 87	-2.16 ± 0.03	16.9 ± 0.5	M4.5
201661761	C14	12.89	7.26 ± 0.10	0.28 ± 0.01	0.28 ± 0.01	3160 ± 83	-2.11 ± 0.04	21.3 ± 1.0	M4.5
201703096	C14	12.01	5.06 ± 0.06	0.60 ± 0.02	0.62 ± 0.02	3767 ± 83	-1.14 ± 0.03	57.5 ± 1.7	M0.5
201705990	C14	12.04	6.14 ± 0.12	0.42 ± 0.02	0.44 ± 0.02	3496 ± 91	-1.62 ± 0.05	28.6 ± 1.6	M2.5
201820874	C14	12.14	5.04 ± 0.05	0.60 ± 0.02	0.63 ± 0.01	3797 ± 81	-1.13 ± 0.03	62.5 ± 1.6	M0.5
248425357	C14	12.04	4.65 ± 0.06	0.68 ± 0.02	0.69 ± 0.02	3998 ± 85	-0.95 ± 0.03	77.4 ± 2.3	M0.0
248432941	C14	8.77	5.92 ± 0.13	0.46 ± 0.02	0.48 ± 0.02	3505 ± 86	-1.52 ± 0.05	7.6 ± 0.5	M2.5
248453031	C14	11.07	5.13 ± 0.07	0.59 ± 0.02	0.61 ± 0.02	3759 ± 89	-1.17 ± 0.03	36.3 ± 1.3	M0.5
248468115	C14	11.87	5.09 ± 0.06	0.59 ± 0.02	0.62 ± 0.02	3790 ± 82	-1.15 ± 0.03	54.0 ± 1.6	M0.5
248473036	C14	12.55	6.25 ± 0.05	0.41 ± 0.01	0.42 ± 0.01	3455 ± 81	-1.67 ± 0.03	35.0 ± 0.9	M3.0
248504645	C14	11.82	5.12 ± 0.07	0.59 ± 0.02	0.61 ± 0.02	3745 ± 87	-1.17 ± 0.03	50.3 ± 1.8	M0.5
248505702	C14	10.89	5.78 ± 0.05	0.48 ± 0.02	0.50 ± 0.01	3598 ± 84	-1.46 ± 0.03	21.7 ± 0.6	M2.0
248601792	C14	13.34	8.17 ± 0.08	0.20 ± 0.01	0.19 ± 0.01	3038 ± 80	-2.50 ± 0.03	14.3 ± 0.5	M5.5
248637069	C14	10.44	7.23 ± 0.08	0.29 ± 0.01	0.29 ± 0.01	3257 ± 87	-2.09 ± 0.03	6.7 ± 0.2	M4.5
248664460	C14	11.82	5.08 ± 0.06	0.60 ± 0.02	0.62 ± 0.02	3789 ± 89	-1.15 ± 0.03	53.1 ± 1.6	M0.5
248698478	C14	11.49	4.86 ± 0.05	0.64 ± 0.02	0.66 ± 0.01	3940 ± 85	-1.05 ± 0.03	53.4 ± 1.3	M0.0
248759329	C14	12.36	6.81 ± 0.06	0.33 ± 0.01	0.34 ± 0.01	3327 ± 82	-1.91 ± 0.03	22.7 ± 0.7	M3.5
248775337	C14	12.71	6.73 ± 0.05	0.34 ± 0.01	0.35 ± 0.01	3303 ± 80	-1.88 ± 0.03	28.1 ± 0.7	M3.5
248804846	C14	11.13	4.09 ± 0.05	0.79 ± 0.03	0.78 ± 0.02	4180 ± 84	-0.69 ± 0.02	76.3 ± 1.9	K6.0
248826058	C14	12.31	6.15 ± 0.05	0.42 ± 0.01	0.44 ± 0.01	3437 ± 80	-1.62 ± 0.03	34.1 ± 0.9	M2.5
248849485	C14	11.80	4.69 ± 0.06	0.67 ± 0.02	0.69 ± 0.02	3912 ± 83	-0.97 ± 0.03	68.6 ± 2.0	M0.0
248856749	C14	12.27	5.82 ± 0.09	0.47 ± 0.02	0.49 ± 0.02	3539 ± 83	-1.48 ± 0.04	40.3 ± 1.7	M2.0
248857979	C14	10.96	4.68 ± 0.06	0.67 ± 0.02	0.69 ± 0.02	3943 ± 90	-0.97 ± 0.03	47.1 ± 1.4	M0.0
248870284	C14	12.34	6.83 ± 0.06	0.33 ± 0.01	0.34 ± 0.01	3354 ± 80	-1.92 ± 0.03	22.1 ± 0.7	M3.5
249101965	C15	12.52	6.76 ± 0.06	0.34 ± 0.01	0.35 ± 0.01	3374 ± 85	-1.89 ± 0.03	25.0 ± 0.7	M3.5
249186244	C15	12.41	6.04 ± 0.05	0.44 ± 0.01	0.46 ± 0.01	3458 ± 80	-1.57 ± 0.03	39.3 ± 1.0	M2.5
249328859	C15	10.93	5.19 ± 0.06	0.58 ± 0.02	0.60 ± 0.01	3711 ± 86	-1.20 ± 0.03	33.6 ± 0.9	M1.0
249338840	C15	10.99	5.70 ± 0.06	0.49 ± 0.02	0.51 ± 0.01	3590 ± 82	-1.42 ± 0.03	24.4 ± 0.7	M2.0
249591902	C15	12.40	5.48 ± 0.06	0.53 ± 0.02	0.55 ± 0.01	3633 ± 83	-1.33 ± 0.03	54.1 ± 1.6	M1.5
249655888	C15	11.55	4.79 ± 0.13	0.65 ± 0.03	0.67 ± 0.03	3912 ± 99	-1.02 ± 0.05	56.8 ± 3.4	M0.0
249677429	C15	12.15	6.48 ± 0.06	0.38 ± 0.01	0.39 ± 0.01	3436 ± 83	-1.77 ± 0.03	25.0 ± 0.7	M3.0
249680584	C15	12.62	6.42 ± 0.06	0.38 ± 0.01	0.40 ± 0.01	3352 ± 83	-1.74 ± 0.03	34.4 ± 1.1	M3.0
249681555	C15	11.94	6.55 ± 0.05	0.37 ± 0.01	0.38 ± 0.01	3317 ± 82	-1.80 ± 0.02	13.3 ± 0.3	M3.5
249860217	C15	10.89	5.68 ± 0.09	0.49 ± 0.02	0.52 ± 0.02	3641 ± 84	-1.42 ± 0.04	23.4 ± 1.0	M2.0
249899499	C15	11.96	5.02 ± 0.06	0.61 ± 0.02	0.63 ± 0.01	3767 ± 84	-1.12 ± 0.03	59.8 ± 1.7	M0.5
250022000	C15	11.77	4.96 ± 0.06	0.62 ± 0.02	0.64 ± 0.02	3831 ± 85	-1.09 ± 0.03	58.4 ± 1.7	M0.5
250034723	C15	11.06	4.51 ± 0.04	0.71 ± 0.02	0.72 ± 0.01	4027 ± 85	-0.89 ± 0.02	54.7 ± 1.2	K7.0
250053801	C15	12.03	4.96 ± 0.07	0.62 ± 0.02	0.64 ± 0.02	3854 ± 85	-1.09 ± 0.03	62.8 ± 2.2	M0.5
250072828	C15	12.16	5.61 ± 0.09	0.51 ± 0.02	0.53 ± 0.02	3610 ± 84	-1.38 ± 0.04	43.5 ± 1.9	M2.0
250111823	C15	11.51	7.10 ± 0.09	0.30 ± 0.01	0.30 ± 0.01	3247 ± 84	-2.04 ± 0.04	12.4 ± 0.5	M4.0
250122612	C15	11.30	4.28 ± 0.04	0.75 ± 0.02	0.75 ± 0.02	4135 ± 83	-0.78 ± 0.02	70.2 ± 1.5	K7.0

to be continued on the next page

Table A1 continued.

EPIC ID	Camp.	K_p	M_{Ks} mag	R_* [R_\odot]	M_* [M_\odot]	T_{eff}^* [K]	$\log L_{\text{bol}}$ [L_\odot]	d [pc]	SpT
211400445	C16	9.80	5.59 ± 0.07	0.51 ± 0.02	0.53 ± 0.02	3563 ± 83	-1.37 ± 0.03	15.1 ± 0.5	M1.5
211456957	C16	10.44	4.56 ± 0.06	0.70 ± 0.02	0.71 ± 0.02	3994 ± 83	-0.91 ± 0.03	40.6 ± 1.2	K7.0
211467243	C16	13.04	8.02 ± 0.09	0.21 ± 0.01	0.20 ± 0.01	3064 ± 81	-2.44 ± 0.04	13.7 ± 0.6	M5.5
211489708	C16	11.53	5.79 ± 0.07	0.48 ± 0.02	0.50 ± 0.02	3592 ± 86	-1.46 ± 0.03	28.6 ± 1.0	M2.0
211516815	C16	12.06	4.98 ± 0.05	0.61 ± 0.02	0.64 ± 0.01	3802 ± 81	-1.10 ± 0.03	63.8 ± 1.6	M0.5
211616023	C16	10.78	4.78 ± 0.06	0.65 ± 0.02	0.67 ± 0.02	3945 ± 97	-1.01 ± 0.03	39.9 ± 1.2	M0.0
211630934	C16	10.38	4.93 ± 0.06	0.62 ± 0.02	0.65 ± 0.02	3840 ± 83	-1.08 ± 0.03	30.3 ± 0.9	M0.0
211736506	C16	10.84	9.46 ± 0.26	0.13 ± 0.01	0.15 ± 0.00	2848 ± 135	-3.05 ± 0.10	6.1 ± 0.8	M7.5
211832386	C16	12.71	7.06 ± 0.09	0.30 ± 0.01	0.31 ± 0.01	3284 ± 81	-2.02 ± 0.04	22.1 ± 0.9	M4.0
211857745	C16	10.69	5.48 ± 0.06	0.53 ± 0.02	0.55 ± 0.01	3612 ± 82	-1.33 ± 0.03	25.7 ± 0.8	M1.5
211864396	C16	11.89	6.81 ± 0.06	0.33 ± 0.01	0.34 ± 0.01	3345 ± 82	-1.91 ± 0.03	18.0 ± 0.6	M3.5
211890761	C16	11.64	4.43 ± 0.04	0.72 ± 0.02	0.73 ± 0.01	4039 ± 81	-0.85 ± 0.02	76.5 ± 1.7	K7.0
211892034	C5,C16	11.58	6.03 ± 0.07	0.44 ± 0.02	0.46 ± 0.01	3459 ± 88	-1.57 ± 0.03	26.4 ± 0.9	M2.5
212038542	C16	11.40	4.54 ± 0.07	0.70 ± 0.02	0.71 ± 0.02	4033 ± 87	-0.90 ± 0.03	62.7 ± 2.2	K7.0
212093841	C16	12.02	6.18 ± 0.16	0.42 ± 0.03	0.43 ± 0.03	3490 ± 91	-1.64 ± 0.07	29.8 ± 2.2	M2.5
251282832	C16	12.47	6.54 ± 0.06	0.37 ± 0.01	0.38 ± 0.01	3404 ± 83	-1.79 ± 0.03	27.5 ± 0.8	M3.0
251341401	C16	11.49	4.84 ± 0.14	0.64 ± 0.03	0.66 ± 0.03	3882 ± 98	-1.04 ± 0.06	53.3 ± 3.6	M0.0
212405060	C6,C17	12.50	6.45 ± 0.06	0.38 ± 0.01	0.39 ± 0.01	3427 ± 80	-1.75 ± 0.03	29.0 ± 0.9	M3.0
212424143	C6,C17	12.01	6.76 ± 0.08	0.34 ± 0.01	0.35 ± 0.01	3351 ± 87	-1.89 ± 0.03	19.4 ± 0.7	M3.5
212438743	C6,C17	11.06	5.07 ± 0.05	0.60 ± 0.02	0.62 ± 0.01	3775 ± 82	-1.14 ± 0.03	39.5 ± 1.0	M0.5
212518629	C6,C17	12.46	6.89 ± 0.06	0.32 ± 0.01	0.33 ± 0.01	3302 ± 80	-1.95 ± 0.03	22.4 ± 0.7	M4.0
212518679	C17	12.16	5.11 ± 0.08	0.59 ± 0.02	0.61 ± 0.02	3806 ± 87	-1.16 ± 0.04	59.2 ± 2.3	M0.5
212556566	C6,C17	12.86	7.49 ± 0.06	0.26 ± 0.01	0.25 ± 0.01	3204 ± 82	-2.21 ± 0.03	18.4 ± 0.6	M4.5
212560714	C6,C17	11.27	4.74 ± 0.06	0.66 ± 0.02	0.68 ± 0.02	3906 ± 93	-0.99 ± 0.03	52.1 ± 1.5	M0.0
212578572	C6,C17	12.06	4.68 ± 0.09	0.67 ± 0.03	0.69 ± 0.02	3961 ± 87	-0.97 ± 0.04	79.0 ± 3.2	M0.0
212610229	C17	11.75	6.38 ± 0.06	0.39 ± 0.01	0.40 ± 0.01	3394 ± 81	-1.72 ± 0.03	30.9 ± 0.9	M3.0
212611828	C6,C17	12.85	6.56 ± 0.09	0.37 ± 0.02	0.38 ± 0.02	3343 ± 84	-1.80 ± 0.04	32.4 ± 1.5	M3.5
212652474	C17	12.00	4.77 ± 0.07	0.66 ± 0.02	0.67 ± 0.02	3907 ± 87	-1.00 ± 0.03	71.3 ± 2.4	M0.0
212662886	C17	11.66	5.40 ± 0.06	0.54 ± 0.02	0.56 ± 0.01	3717 ± 89	-1.29 ± 0.03	40.0 ± 1.2	M1.5
212663959	C6,C17	12.23	6.46 ± 0.05	0.38 ± 0.01	0.39 ± 0.01	3361 ± 81	-1.76 ± 0.03	27.7 ± 0.8	M3.0
212679181	C6,C17	12.01	5.94 ± 0.08	0.45 ± 0.02	0.47 ± 0.02	3512 ± 84	-1.53 ± 0.04	33.8 ± 1.3	M2.5
212681560	C6,C17	11.91	6.27 ± 0.05	0.40 ± 0.01	0.42 ± 0.01	3443 ± 83	-1.68 ± 0.03	26.7 ± 0.7	M3.0
212681564	C6,C17	11.82	8.69 ± 0.31	0.16 ± 0.02	0.16 ± 0.01	2942 ± 97	-2.72 ± 0.13	10.3 ± 1.5	M6.5
212710520	C6,C17	11.72	4.84 ± 0.07	0.64 ± 0.02	0.66 ± 0.02	3914 ± 87	-1.04 ± 0.03	60.2 ± 2.0	M0.0
212712577	C6,C17	10.86	4.68 ± 0.05	0.67 ± 0.02	0.69 ± 0.01	3933 ± 88	-0.96 ± 0.02	44.3 ± 1.2	M0.0
212712579	C17	10.88	4.68 ± 0.05	0.67 ± 0.02	0.69 ± 0.02	3933 ± 87	-0.96 ± 0.02	44.3 ± 1.2	M0.0
212734783	C17	11.60	6.34 ± 0.13	0.40 ± 0.02	0.41 ± 0.02	3415 ± 87	-1.71 ± 0.05	21.0 ± 1.3	M3.0
212776174	C6,C17	10.03	4.87 ± 0.04	0.64 ± 0.02	0.66 ± 0.01	3855 ± 87	-1.05 ± 0.02	27.4 ± 0.7	M0.0
212807182	C6,C17	12.23	5.61 ± 0.09	0.51 ± 0.02	0.53 ± 0.02	3583 ± 83	-1.39 ± 0.04	46.7 ± 1.9	M2.0
212810669	C6,C17	12.54	6.24 ± 0.08	0.41 ± 0.02	0.43 ± 0.02	3445 ± 84	-1.66 ± 0.04	35.9 ± 1.5	M3.0
212840848	C17	8.91	4.76 ± 0.09	0.66 ± 0.03	0.68 ± 0.02	3919 ± 99	-1.00 ± 0.04	18.0 ± 0.7	M0.0
212846068	C17	11.24	5.09 ± 0.09	0.60 ± 0.02	0.62 ± 0.02	3813 ± 88	-1.15 ± 0.04	40.0 ± 1.8	M0.5
212874829	C17	11.85	5.28 ± 0.09	0.56 ± 0.02	0.59 ± 0.02	3742 ± 88	-1.24 ± 0.04	47.8 ± 2.0	M1.0
251512053	C17	10.65	4.98 ± 0.06	0.61 ± 0.02	0.64 ± 0.02	3870 ± 85	-1.10 ± 0.03	32.3 ± 1.0	M0.5
251540467	C17	11.49	5.09 ± 0.07	0.59 ± 0.02	0.62 ± 0.02	3817 ± 91	-1.15 ± 0.03	43.4 ± 1.5	M0.5
251550724	C17	10.16	6.26 ± 0.05	0.41 ± 0.01	0.42 ± 0.01	3448 ± 86	-1.67 ± 0.03	11.8 ± 0.3	M3.0
251567386	C17	12.31	5.84 ± 0.20	0.47 ± 0.03	0.49 ± 0.04	3570 ± 94	-1.49 ± 0.08	41.0 ± 3.9	M2.0
251583820	C17	12.44	6.42 ± 0.08	0.38 ± 0.02	0.40 ± 0.01	3400 ± 81	-1.74 ± 0.03	29.6 ± 1.1	M3.0
251584738	C17	10.91	5.42 ± 0.06	0.54 ± 0.02	0.56 ± 0.01	3660 ± 84	-1.30 ± 0.03	26.4 ± 0.8	M1.5
211364964	C5,C18	12.01	4.62 ± 0.07	0.68 ± 0.02	0.70 ± 0.02	3956 ± 86	-0.94 ± 0.03	79.7 ± 2.9	M0.0
211385897	C5,C18	11.67	4.60 ± 0.05	0.69 ± 0.02	0.70 ± 0.02	3958 ± 82	-0.93 ± 0.02	67.9 ± 1.8	K7.0
211427097	C5,C16 C18	11.73	4.05 ± 0.19	0.80 ± 0.05	0.79 ± 0.03	4263 ± 136	-0.67 ± 0.08	104.6 ± 9.1	K6.0
211480655	C5,C16 C18	12.21	6.89 ± 0.15	0.32 ± 0.02	0.33 ± 0.02	3320 ± 88	-1.95 ± 0.06	19.6 ± 1.3	M4.0
211481688	C5,C16 C18	11.81	4.76 ± 0.33	0.66 ± 0.07	0.67 ± 0.06	3893 ± 156	-1.00 ± 0.13	66.7 ± 10.0	M0.0

to be continued on the next page

Table A1 continued.

EPIC ID	Camp.	K_p	M_{Ks} mag	R_* [R_\odot]	M_* [M_\odot]	T_{eff}^* [K]	$\log L_{\text{bol}}$ [L_\odot]	d [pc]	SpT
211498244	C5,C18	11.88	5.32 ± 0.06	0.55 ± 0.02	0.58 ± 0.01	3679 ± 82	-1.26 ± 0.03	46.2 ± 1.4	M1.0
211599658	C5,C18	12.02	5.44 ± 0.10	0.53 ± 0.02	0.56 ± 0.02	3683 ± 84	-1.31 ± 0.04	46.0 ± 2.2	M1.5
211642294	C5,C18	10.79	6.20 ± 0.09	0.41 ± 0.02	0.43 ± 0.02	3422 ± 88	-1.65 ± 0.04	16.7 ± 0.7	M2.5
211788733	C5,C18	11.95	5.02 ± 0.12	0.61 ± 0.03	0.63 ± 0.02	3785 ± 88	-1.12 ± 0.05	60.1 ± 3.2	M0.5
211845940	C5,C16 C18	11.87	5.51 ± 0.07	0.52 ± 0.02	0.55 ± 0.02	3643 ± 84	-1.34 ± 0.03	40.5 ± 1.4	M1.5
211889233	C5,C16 C18	11.59	4.91 ± 0.05	0.63 ± 0.02	0.65 ± 0.01	3883 ± 81	-1.07 ± 0.03	53.0 ± 1.3	M0.0
211944670	C18	10.55	7.11 ± 0.08	0.30 ± 0.01	0.30 ± 0.01	3282 ± 80	-2.04 ± 0.03	7.9 ± 0.3	M4.0
211944676	C5,C18	9.90	7.11 ± 0.08	0.30 ± 0.01	0.30 ± 0.01	3282 ± 80	-2.04 ± 0.03	7.9 ± 0.3	M4.0
211944856	C5,C18	11.02	9.25 ± 0.31	0.13 ± 0.01	0.15 ± 0.01	2869 ± 93	-2.96 ± 0.13	4.9 ± 0.7	M7.5
211945363	C5,C16 C18	12.35	6.73 ± 0.06	0.34 ± 0.01	0.35 ± 0.01	3334 ± 81	-1.88 ± 0.03	23.7 ± 0.7	M3.5
211992989	C5,C18	12.80	6.20 ± 0.05	0.41 ± 0.01	0.43 ± 0.01	3411 ± 79	-1.65 ± 0.02	31.3 ± 0.7	M2.5
212162615	C5,C16 C18	12.61	6.47 ± 0.06	0.38 ± 0.01	0.39 ± 0.01	3451 ± 80	-1.76 ± 0.03	28.2 ± 0.9	M3.0
212171836	C5,C18	11.65	5.43 ± 0.08	0.53 ± 0.02	0.56 ± 0.02	3694 ± 90	-1.31 ± 0.04	38.9 ± 1.6	M1.5
246001292	C12,C19	11.86	4.26 ± 0.05	0.76 ± 0.02	0.76 ± 0.02	4156 ± 85	-0.77 ± 0.03	91.9 ± 2.5	K7.0
246033148	C19	12.17	7.14 ± 0.07	0.29 ± 0.01	0.30 ± 0.01	3269 ± 82	-2.05 ± 0.03	25.0 ± 0.9	M4.0
246079058	C19	12.05	5.06 ± 0.04	0.60 ± 0.02	0.62 ± 0.01	3820 ± 80	-1.14 ± 0.02	57.2 ± 1.3	M0.5
246093819	C19	12.28	6.32 ± 0.05	0.40 ± 0.01	0.41 ± 0.01	3457 ± 80	-1.70 ± 0.02	28.7 ± 0.7	M3.0
246132735	C12,C19	13.10	7.68 ± 0.05	0.24 ± 0.01	0.23 ± 0.01	3186 ± 80	-2.29 ± 0.02	17.6 ± 0.4	M5.0
246141580	C19	12.17	6.11 ± 0.05	0.43 ± 0.01	0.45 ± 0.01	3470 ± 80	-1.61 ± 0.02	32.2 ± 0.7	M2.5
246179278	C12,C19	12.52	6.48 ± 0.09	0.38 ± 0.02	0.39 ± 0.02	3418 ± 81	-1.77 ± 0.04	28.8 ± 1.2	M3.0
246182783	C19	12.33	5.55 ± 0.04	0.52 ± 0.02	0.54 ± 0.01	3605 ± 81	-1.36 ± 0.02	49.9 ± 1.1	M1.5
246191912	C12,C19	12.51	6.73 ± 0.05	0.34 ± 0.01	0.35 ± 0.01	3363 ± 80	-1.88 ± 0.02	24.7 ± 0.6	M3.5
246238886	C12,C19	9.91	5.20 ± 0.04	0.58 ± 0.02	0.60 ± 0.01	3769 ± 84	-1.20 ± 0.02	20.3 ± 0.5	M1.0
246301900	C12,C19	10.81	4.67 ± 0.06	0.67 ± 0.02	0.69 ± 0.02	3932 ± 90	-0.96 ± 0.03	44.9 ± 1.4	M0.0
246310210	C19	12.39	5.58 ± 0.04	0.51 ± 0.02	0.53 ± 0.01	3631 ± 80	-1.37 ± 0.02	50.4 ± 1.1	M1.5
246333864	C12,C19	11.67	8.98 ± 0.09	0.15 ± 0.01	0.15 ± 0.00	2956 ± 82	-2.85 ± 0.04	6.9 ± 0.3	M7.0
246364217	C12,C19	12.44	7.17 ± 0.05	0.29 ± 0.01	0.29 ± 0.01	3236 ± 81	-2.07 ± 0.02	18.4 ± 0.4	M4.0
246374497	C12,C19	10.98	5.25 ± 0.06	0.57 ± 0.02	0.59 ± 0.01	3692 ± 85	-1.22 ± 0.03	32.7 ± 0.9	M1.0
246378594	C19	12.71	6.76 ± 0.05	0.34 ± 0.01	0.35 ± 0.01	3360 ± 81	-1.89 ± 0.02	26.9 ± 0.6	M3.5
246379501	C19	11.66	4.76 ± 0.21	0.66 ± 0.04	0.67 ± 0.04	3966 ± 122	-1.00 ± 0.08	55.4 ± 5.3	M0.0
246419402	C12,C19	11.83	5.41 ± 0.04	0.54 ± 0.02	0.56 ± 0.01	3611 ± 81	-1.30 ± 0.02	42.9 ± 1.0	M1.5
246424810	C19	12.20	5.83 ± 0.06	0.47 ± 0.02	0.49 ± 0.01	3589 ± 82	-1.48 ± 0.03	38.2 ± 1.1	M2.0
246446811	C19	12.21	6.47 ± 0.05	0.38 ± 0.01	0.39 ± 0.01	3390 ± 81	-1.76 ± 0.03	25.7 ± 0.7	M3.0
246461560	C12,C19	11.29	5.27 ± 0.06	0.56 ± 0.02	0.59 ± 0.01	3725 ± 86	-1.23 ± 0.03	37.1 ± 1.0	M1.0
251718998	C19	11.76	5.05 ± 0.04	0.60 ± 0.02	0.63 ± 0.01	3868 ± 91	-1.13 ± 0.02	51.5 ± 1.1	M0.5
251728337	C19	10.36	4.51 ± 0.04	0.71 ± 0.02	0.72 ± 0.01	4031 ± 83	-0.89 ± 0.02	40.0 ± 0.9	K7.0

Table A2: Rotation period and activity indicators for all 430 targets. For the 48 targets that were observed in multiple campaigns the LC of each campaign was analyzed individually. Method: method that yielded best period selected by eye-inspection. Flag: reliability of determined periods. ν : Flare frequency. We consider all periods greater than half the campaign duration as periods with less confidence. For periods larger than the campaign duration we do not give any uncertainties as they are the ones with the lowest confidence.

EPIC ID	Camp.	P_{rot} [d]	Method	Flag	R_{per} [%]	S_{ph} [ppm]	S_{flat} [ppm]	N_{Flares}	ν [N_{flares}/d]
202059183	C0	—	—	N	—	607.99	135.14	0	—
202059188	C0	0.691 ± 0.000	LS	Y	2.525 ± 0.202	10520.91	2504.63	4	0.121
202059190	C0	—	—	N	—	1012.63	93.06	0	—
202059192	C0	35.220 ± 1.169	SINE	?	0.468 ± 0.051	1844.13	105.82	0	—
202059193	C0	19.012 ± 1.046	LS	?	0.403 ± 0.071	1161.41	111.35	0	—

to be continued on the next page

Table A2 continued.

EPIC ID	Camp.	P_{tot} [d]	Method	Flag	R_{per} [%]	S_{ph} [ppm]	S_{flat} [ppm]	N_{Flares}	ν [N_{flares}/d]
202059195	C0	42.460 ±	SINE	?	1.707 ± 0.805	6447.70	161.18	0	—
202059197	C0	—	—	N	—	1070.55	80.90	0	—
202059198	C0	27.307 ± 0.465	LS	?	0.830 ± 0.029	2802.33	80.49	1	0.030
202059199	C0	—	—	N	—	2507.98	94.74	4	0.121
202059203	C0	—	—	N	—	635.64	117.52	0	—
202059204	C0	7.887 ± 0.070	ACF	Y	2.513 ± 0.126	8494.33	321.07	3	0.091
202059207	C0	15.160 ± 0.371	ACF	Y	0.088 ± 0.035	386.84	74.76	1	0.030
202059208	C0	—	—	N	—	1534.31	95.53	0	—
202059210	C0	17.796 ± 0.410	LS	?	1.252 ± 0.144	4813.81	126.01	0	—
202059215	C0	—	—	N	—	2021.97	161.14	3	0.091
202059221	C0	—	—	N	—	739.35	119.31	0	—
202059222	C0	72.160 ±	SINE	?	1.272 ± 0.280	4496.08	148.43	0	—
202059223	C0	—	—	N	—	294.01	138.82	0	—
202059224	C0	—	—	N	—	1008.82	83.02	0	—
202059229	C0	5.006 ± 0.025	ACF	Y	2.401 ± 0.247	7218.59	568.42	4	0.121
202059231	C0	17.425 ± 0.772	LS	?	3.005 ± 0.379	11047.20	284.24	10	0.302
202059243	C0	—	—	N	—	1239.99	99.09	1	0.030
201237257	C1	31.690 ± 0.763	ACF	Y	2.523 ± 0.067	7330.47	83.00	3	0.037
201323410	C1	73.860 ± 1.590	SINE	?	0.956 ± 0.140	3192.96	104.11	2	0.025
201364753	C1	9.291 ± 0.141	LS	Y	0.369 ± 0.021	2224.37	69.31	0	—
201367065	C1	38.861 ± 0.655	ACF	Y	0.200 ± 0.152	779.95	86.52	0	—
201460770	C1	20.268* ± 0.320	ACF	Y	0.366 ± 0.329	2576.88	76.49	2	0.025
201481218	C1	32.037 ± 0.386	ACF	Y	0.254 ± 0.071	1659.18	54.99	2	0.025
201482319	C1	11.676 ± 0.111	LS	Y	4.829 ± 6.489	17064.27	937.50	21	0.262
201497866	C1	42.226 ± 1.219	LS	?	0.311 ± 0.164	1365.28	86.52	0	—
201498184	C1	—	—	N	—	4011.39	78.52	0	—
201506253	C1	32.384 ± 0.640	ACF	?	1.397 ± 0.039	4439.16	67.64	2	0.025
201518346	C1	112.830 ±	SINE	?	1.142 ± 0.091	4012.55	83.05	6	0.075
201568682	C1	38.935 ± 1.464	LS	?	1.076 ± 0.064	3892.25	94.52	0	—
201597919	C1	40.847 ± 0.905	LS	Y	0.500 ± 0.125	1755.07	102.96	4	0.050
201611969	C1	25.992 ± 0.850	LS	?	0.670 ± 0.046	3811.80	71.60	7	0.087
201675315	C1	38.126 ± 1.349	ACF	Y	0.506 ± 0.059	2551.77	61.75	2	0.025
201717312	C1	34.142 ± 0.840	ACF	Y	0.636 ± 0.037	1961.90	100.30	0	—
201717791	C1	15.048 ± 0.401	LS	Y	0.117 ± 0.038	511.28	97.92	1	0.012
201718613	C1	78.960 ± 0.750	SINE	?	1.083 ± 0.078	3485.26	111.38	7	0.087
201719115	C1	36.001 ± 0.649	ACF	Y	0.751 ± 0.037	2551.80	74.44	2	0.025
201719818	C1	29.687 ± 0.753	ACF	?	0.523 ± 0.023	1562.58	51.80	0	—
201779048	C1	25.805 ± 0.542	ACF	Y	0.225 ± 0.058	1626.83	70.08	2	0.025
201806997	C1	0.656 ± 0.000	LS	Y	13.950 ± 1.208	56945.06	10596.36	2	0.025
201842163	C1	0.766 ± 0.002	LS	Y	2.404 ± 0.169	10246.35	1450.11	9	0.112
201867138	C1	37.656 ± 1.241	ACF	Y	0.563 ± 0.058	2358.25	114.32	1	0.012
201909533	C1	2.294 ± 0.003	LS	Y	4.077 ± 0.240	8275.11	1274.78	16	0.200
201912552	C1	40.802 ± 0.859	ACF	Y	1.215 ± 0.087	3995.50	145.65	0	—
201917390	C1	0.708 ± 0.001	LS	Y	2.122 ± 0.137	7179.35	1306.98	15	0.187
202571062	C2	3.988 ± 0.017	LS	Y	5.277 ± 3.784	17420.20	615.80	6	0.077
202748218	C2	120.610 ±	SINE	?	1.134 ± 0.243	2787.07	163.95	0	—
203083752	C2	—	—	N	—	4142.49	236.63	1	0.013
203099398	C2	17.919 ± 0.845	ACF	Y	0.453 ± 0.033	1995.35	76.23	0	—
203124214	C2	7.985 ± 0.005	LS	?	0.100 ± 0.035	1170.01	73.04	0	—
203354308	C2	19.819 ± 0.371	ACF	Y	0.364 ± 0.049	1280.90	66.12	0	—
203740889	C2	59.156 ± 2.044	LS	?	0.825 ± 0.139	3307.29	144.12	0	—
203846654	C2	21.515 ± 0.547	ACF	Y	0.556 ± 0.079	2142.00	100.11	0	—
203869467	C2	46.944 ± 2.191	LS	?	0.950 ± 0.216	3418.82	190.63	0	—
203881088	C2	—	—	N	—	3161.35	161.31	0	—
204080947	C2	29.299 ± 0.359	ACF	Y	0.878 ± 0.105	2961.49	176.89	0	—
204536344	C2	19.594 ± 0.032	ACF	Y	0.625 ± 0.026	2365.36	48.62	1	0.013
204610472	C2	42.559 ± 0.488	ACF	?	0.659 ± 0.108	2183.22	145.87	1	0.013

to be continued on the next page

Table A2 continued.

EPIC ID	Camp.	P_{rot} [d]	Method	Flag	R_{per} [%]	S_{ph} [ppm]	S_{flat} [ppm]	N_{Flares}	ν [N_{flares}/d]
204927969	C2	1.553 ± 0.000	ACF	Y	1.297 ± 0.112	5770.52	1119.94	7	0.090
204957517	C2	2.823 ± 0.001	LS	Y	1.968 ± 0.412	6937.90	1150.43	10	0.129
204963027	C2	14.527 ± 0.028	ACF	Y	1.216 ± 0.043	3459.27	92.83	1	0.013
204976998	C2	—	—	N	—	1384.89	213.69	0	—
204994054	C2	—	—	N	—	2025.03	160.42	0	—
205030726	C2	21.065 ± 1.666	ACF	?	0.196 ± 0.092	1211.07	98.17	1	0.013
205040974	C2	22.373 ± 0.990	ACF	?	0.596 ± 0.062	3064.50	106.66	1	0.013
205182959	C2	46.080 ± 0.340	LS	?	1.445 ± 0.308	2282.09	119.89	0	—
205196227	C2	—	—	N	—	1298.91	61.72	1	0.013
205339436	C2	—	—	N	—	12089.79	303.32	0	—
205467732	C2	1.321 ± 0.010	LS	Y	0.853 ± 0.215	5478.68	801.89	10	0.129
205489894	C2	22.802 ± 1.247	ACF	?	0.545 ± 0.033	2345.86	125.74	1	0.013
205507325	C2	63.870 ± 7.757	ACF	?	1.522 ± 0.284	5079.50	120.08	1	0.013
205536237	C2	19.431 ± 0.345	ACF	Y	0.653 ± 0.128	2093.06	77.62	0	—
205599283	C2	14.568 ± 0.684	ACF	Y	0.503 ± 0.025	1900.60	95.69	0	—
205631193	C2	—	—	N	—	1244.69	224.99	0	—
205913009	C3	116.400 ±	SINE	?	2.410 ± 0.341	8886.18	143.33	1	0.015
205952383	C3	35.017 ± 0.563	LS	?	0.885 ± 0.028	2821.74	48.23	1	0.015
206007536	C3	16.095 ± 0.503	LS	Y	0.555 ± 0.026	3745.53	52.55	2	0.030
206019392	C3	75.440 ±	SINE	?	3.054 ± 0.112	11877.92	43.49	15	0.225
206054454	C3	—	—	N	—	4532.94	87.62	0	—
206055065	C3	—	—	N	—	2273.81	35.27	2	0.030
206056832	C3	—	—	N	—	3200.12	35.27	2	0.030
206107346	C3	—	—	N	—	1230.19	48.36	0	—
206181550	C3	31.099 ± 0.967	LS	Y	0.667 ± 0.049	2003.25	67.56	0	—
206208968	C3	0.710 ± 0.009	LS	Y	0.930 ± 0.184	7936.11	1591.88	6	0.090
206249569	C3	27.661 ± 0.826	LS	Y	0.434 ± 0.031	1295.40	102.14	1	0.015
206262223	C3	9.725 ± 0.015	ACF	Y	4.362 ± 7.527	14531.49	1120.80	17	0.254
206262336	C3	9.705 ± 0.018	ACF	Y	4.368 ± 7.586	14522.43	1122.57	14	0.210
206288689	C3	—	—	N	—	1199.20	71.28	3	0.045
206349327	C3	3.719 ± 0.008	ACF	Y	14.043 ± 0.542	49235.58	2473.55	4	0.060
206368165	C3	40.042 ± 0.763	LS	?	0.194 ± 0.323	622.98	123.11	0	—
206435478	C3	16.056 ± 0.517	LS	Y	0.445 ± 0.069	4304.13	52.28	5	0.076
206479389	C3	66.710 ±	SINE	?	0.957 ± 0.068	3107.37	104.33	3	0.045
206490189	C3	48.014 ± 1.767	ACF	?	1.211 ± 0.051	4142.23	81.41	2	0.030
210317378	C4	26.909 ± 0.202	ACF	Y	1.857 ± 0.124	5941.14	212.48	4	0.058
210340480	C4	—	—	N	—	5896.14	77.02	1	0.015
210360545	C4	—	—	N	—	11199.87	161.14	0	—
210393283	C4	16.626 ± 0.093	LS	?	0.117 ± 0.119	868.50	93.86	0	—
210408563	C4	17.080 ± 0.648	LS	Y	0.519 ± 0.081	4520.66	127.50	5	0.073
210434433	C4	23.278 ± 0.638	LS	Y	0.996 ± 0.260	6318.15	86.83	3	0.044
210434769	C4	—	—	N	—	1571.81	41.49	0	—
210434976	C4	2.552 ± 0.002	LS	Y	15.069 ± 6.113	18013.08	3460.55	13	0.190
210439387	C4	17.809 ± 0.615	LS	Y	0.611 ± 0.109	2475.13	104.09	0	—
210460280	C4	43.744 ± 0.012	ACF	?	0.993 ± 0.046	4259.06	48.23	3	0.044
210466658	C4	—	—	N	—	909.31	121.34	0	—
210486424	C4	—	—	N	—	10536.41	97.24	7	0.102
210489654	C4	—	—	N	—	7309.01	392.06	2	0.029
210497694	C4	—	—	N	—	3470.71	91.33	0	—
210500368	C4	—	—	N	—	1573.54	74.68	0	—
210500658	C4	23.783 ± 2.378	ACF	Y	0.368 ± 0.154	2377.19	63.04	0	—
210502828	C4	34.044 ± 0.241	LS	?	0.374 ± 0.101	1799.34	44.69	0	—
210535241	C4	14.257 ± 0.141	LS	?	0.179 ± 0.029	2057.37	65.84	2	0.029
210579749	C4	11.245 ± 0.081	LS	Y	0.726 ± 0.078	2916.13	43.90	9	0.131
210580056	C4	21.433 ± 0.224	ACF	Y	0.619 ± 0.024	2631.37	31.56	0	—
210585703	C4	—	—	N	—	3294.59	63.96	0	—
210592074	C4	—	—	N	—	3996.39	58.36	1	0.015

to be continued on the next page

Table A2 continued.

EPIC ID	Camp.	P_{rot} [d]	Method	Flag	R_{per} [%]	S_{ph} [ppm]	S_{flat} [ppm]	N_{Flares}	ν [N_{flares}/d]
210613397	C4	1.745 ± 0.065	LS	Y	2.049 ± 0.426	10218.28	774.24	3	0.044
210651981	C4	2.442 ± 0.019	LS	Y	3.596 ± 0.620	12098.26	1948.84	2	0.029
210651981	C13	2.449 ± 0.000	LS	Y	6.590 ± 0.974	21472.75	3258.46	4	0.050
210693497	C4	21.854 ± 0.821	LS	Y	0.906 ± 0.165	7189.58	92.93	0	—
210707811	C4	11.774 ± 0.225	LS	Y	2.242 ± 0.990	13538.16	339.43	15	0.219
210741091	C4	10.950 ± 0.010	LS	Y	5.533 ± 0.488	18099.59	262.56	12	0.175
210741091	C13	11.721 ± 0.415	LS	?	3.093 ± 0.475	10251.50	251.51	10	0.126
210757663	C4	21.923 ± 0.226	ACF	Y	0.575 ± 0.032	1796.75	80.91	0	—
210778181	C4	29.687 ± 1.179	ACF	Y	1.967 ± 0.082	6084.70	53.42	4	0.058
210941195	C4	21.474 ± 0.350	ACF	Y	0.522 ± 0.033	1568.84	101.74	1	0.015
211006744	C4	24.414 ± 1.165	LS	?	0.630 ± 0.204	2665.03	81.76	0	—
211008819	C4	—	—	N	—	1294.33	146.04	0	—
211029843	C4	—	—	N	—	1799.42	102.58	0	—
211036776	C4	20.738 ± 0.151	ACF	Y	1.875 ± 0.059	6248.60	113.75	5	0.073
211107998	C4	16.121 ± 0.205	ACF	Y	2.045 ± 0.230	10639.78	240.95	14	0.204
211111803	C4	12.931 ± 0.086	LS	Y	3.731 ± 0.319	15252.23	260.41	11	0.160
211183696	C4	94.860 ±	SINE	?	2.797 ± 0.123	10401.35	137.25	3	0.044
211364964	C5	28.798 ± 1.264	LS	Y	0.462 ± 0.092	1632.01	96.74	1	0.014
211364964	C18	26.970 ± 0.472	ACF	?	1.136 ± 0.057	3696.16	103.02	1	0.020
211385897	C5	11.752 ± 0.428	LS	Y	0.492 ± 0.127	6621.20	173.66	13	0.176
211385897	C18	10.992 ± 0.259	ACF	Y	1.053 ± 0.166	3041.70	166.66	13	0.264
211427097	C5	37.411 ± 1.152	LS	?	0.507 ± 0.140	2302.77	71.72	0	—
211427097	C16	35.149 ± 1.130	ACF	Y	0.387 ± 0.098	1306.31	86.40	1	0.013
211427097	C18	16.694* ± 0.013	LS	Y	0.301 ± 0.065	834.89	82.35	0	—
211480655	C5	73.861 ±	LS	?	1.534 ± 0.101	5647.95	114.93	0	—
211480655	C16	87.141 ±	SINE	?	0.809 ± 0.122	2744.72	104.02	1	0.013
211480655	C18	—	—	N	—	6394.19	121.24	0	—
211481688	C5	18.828 ± 0.975	LS	?	0.091 ± 0.114	1681.07	94.14	0	—
211481688	C16	—	—	N	—	1627.28	93.11	0	—
211481688	C18	—	—	N	—	6672.99	98.56	0	—
211498244	C5	—	—	N	—	5898.68	79.99	1	0.014
211498244	C18	—	—	N	—	1510.72	95.68	0	—
211599658	C5	—	—	N	—	1508.03	64.81	1	0.014
211599658	C18	37.962 ± 0.108	ACF	?	0.295 ± 0.041	950.82	72.53	0	—
211642294	C5	—	—	N	—	7175.45	40.53	10	0.135
211642294	C18	47.301 ± 1.083	LS	?	1.469 ± 0.214	4890.63	55.14	11	0.224
211788733	C5	—	—	N	—	898.00	40.53	10	0.135
211788733	C18	—	—	N	—	619.65	78.90	0	—
211845940	C5	—	—	N	—	3645.25	61.19	0	—
211845940	C16	20.185 ± 0.410	LS	Y	0.801 ± 0.114	2861.00	66.95	1	0.013
211845940	C18	—	—	N	—	2671.98	64.27	0	—
211889233	C5	10.517 ± 0.056	LS	Y	1.742 ± 0.515	5339.64	192.70	9	0.122
211889233	C16	10.823 ± 0.065	LS	Y	4.190 ± 0.457	11751.77	206.19	5	0.064
211889233	C18	10.699 ± 0.050	LS	Y	1.926 ± 0.160	5984.82	205.97	4	0.081
211892034	C5	40.434 ± 2.250	LS	?	0.621 ± 0.237	2309.94	66.86	0	—
211892034	C16	37.828 ± 0.242	LS	Y	1.038 ± 0.238	3548.31	54.04	0	—
211944676	C5	—	—	N	—	25485.40	66.86	0	—
211944676	C18	2.773 ± 0.002	SINE	Y	3.986 ± 3.394	9943.83	1687.10	6	0.122
211944856	C5	—	—	N	—	20295.41	1456.75	4	0.054
211944856	C18	2.773 ± 0.002	SINE	Y	3.878 ± 3.842	9683.71	1837.10	6	0.122
211945363	C5	71.743 ± 1.610	LS	?	1.125 ± 0.057	3942.24	81.37	4	0.054
211945363	C16	98.692 ±	SINE	?	4.109 ± 0.138	15959.69	89.61	10	0.128
211945363	C18	44.763 ± 2.472	LS	?	0.840 ± 0.068	2880.12	95.20	4	0.081
211992989	C5	—	—	N	—	603.37	81.37	4	0.054
211992989	C18	—	—	N	—	751.32	95.20	4	0.081
212162615	C5	4.122 ± 0.002	LS	Y	3.754 ± 0.330	13741.30	897.37	16	0.217
212162615	C16	4.138 ± 0.013	SINE	Y	6.875 ± 18.529	20911.89	2704.29	6	0.077

to be continued on the next page

Table A2 continued.

EPIC ID	Camp.	P_{rot} [d]	Method	Flag	R_{per} [%]	S_{ph} [ppm]	S_{flat} [ppm]	N_{Flares}	ν [N_{flares}/d]
212162615	C18	4.123 ± 0.011	LS	Y	6.417 ± 0.687	19592.82	1699.92	9	0.183
212171836	C5	19.263 ± 0.349	LS	?	0.526 ± 0.234	5380.82	92.39	1	0.014
212171836	C18	20.452 ± 0.132	ACF	Y	2.467 ± 0.523	7022.20	101.81	2	0.041
212270936	C6	13.606 ± 0.045	LS	Y	1.351 ± 0.161	5146.36	205.88	8	0.102
212276489	C6	32.547 ± 0.586	LS	?	0.729 ± 0.185	3695.06	96.68	4	0.051
212280999	C6	—	—	N	—	4510.43	96.68	4	0.051
212285603	C6	—	—	N	—	5063.23	49.46	3	0.038
212318785	C6	27.532 ± 1.912	LS	?	1.666 ± 0.647	4542.11	129.28	2	0.025
212323908	C6	—	—	N	—	3929.03	147.75	0	—
212329328	C6	—	—	N	—	1036.00	58.70	0	—
212405060	C6	47.325 ± 0.403	LS	?	0.989 ± 0.049	5225.51	89.82	2	0.025
212405060	C17	46.961 ± 1.196	ACF	?	2.317 ± 0.101	6961.73	164.21	1	0.015
212422696	C6	1.294 ± 0.012	LS	Y	3.966 ± 0.355	12540.38	2493.95	6	0.076
212424143	C6	6.603 ± 0.039	LS	Y	1.400 ± 0.861	5546.13	1045.63	13	0.166
212424143	C17	6.631 ± 0.003	LS	Y	2.090 ± 0.576	7104.03	712.79	6	0.092
212438743	C6	—	—	N	—	847.65	46.65	0	—
212438743	C17	—	—	N	—	2510.85	81.47	0	—
212518629	C6	—	—	N	—	4721.76	105.94	2	0.025
212518629	C17	77.541 ±	SINE	?	1.710 ± 0.248	5522.34	133.69	1	0.015
212556566	C6	1.020 ± 0.010	LS	Y	1.411 ± 0.063	9599.90	1512.24	14	0.178
212556566	C17	1.020 ± 0.022	LS	Y	4.565 ± 1.359	13444.99	1752.93	8	0.122
212557255	C6	8.484* ± 0.054	LS	Y	0.559 ± 0.094	2437.19	74.97	12	0.153
212560714	C6	27.532 ± 0.251	LS	Y	0.361 ± 0.018	1341.53	49.54	1	0.013
212560714	C17	26.321 ± 1.514	ACF	Y	0.443 ± 0.104	1273.27	52.29	1	0.015
212578572	C6	18.971* ± 0.717	LS	Y	0.347 ± 0.022	1308.92	69.38	0	—
212578572	C17	32.803 ± 0.450	LS	Y	1.000 ± 0.173	3165.85	104.36	0	—
212611828	C6	1.096 ± 0.000	LS	Y	2.414 ± 0.388	5698.53	1533.65	19	0.242
212611828	C17	1.094 ± 0.041	LS	Y	4.666 ± 1.161	15054.56	1756.26	8	0.122
212647740	C6	48.238 ± 4.371	LS	?	0.410 ± 0.378	1604.96	98.38	1	0.013
212663915	C6	—	—	N	—	2871.13	68.85	3	0.038
212663959	C6	—	—	N	—	2259.58	73.28	1	0.013
212663959	C17	—	—	N	—	4835.44	83.73	0	—
212679181	C6	33.869 ± 0.241	LS	Y	0.599 ± 0.154	2932.40	79.81	9	0.115
212679181	C17	32.378 ± 1.126	LS	Y	1.313 ± 0.341	3985.42	87.10	8	0.122
212681560	C6	33.869 ± 0.828	LS	Y	0.644 ± 0.089	2392.90	78.12	1	0.013
212681560	C17	33.686 ± 0.514	LS	?	1.018 ± 0.349	3635.25	83.06	5	0.076
212681564	C6	61.224 ± 0.459	LS	?	0.864 ± 0.280	2875.91	149.31	2	0.025
212681564	C17	66.364 ±	SINE	?	0.815 ± 0.267	2975.46	83.06	5	0.076
212710520	C6	—	—	N	—	2326.24	72.76	4	0.051
212710520	C17	—	—	N	—	3388.15	56.71	1	0.015
212712577	C6	13.459* ± 0.153	LS	Y	0.235 ± 0.168	1607.63	51.95	0	—
212712577	C17	29.509 ± 0.220	ACF	?	0.675 ± 0.106	1999.20	50.47	1	0.015
212776174	C6	18.015 ± 0.369	LS	Y	0.619 ± 0.060	2193.01	46.15	1	0.013
212776174	C17	18.474 ± 0.091	ACF	Y	0.585 ± 0.044	1778.07	32.49	5	0.076
212807182	C6	35.303 ± 0.159	LS	Y	0.692 ± 0.225	2369.74	118.16	1	0.013
212807182	C17	19.393 ± 1.024	ACF	?	0.924 ± 0.281	2816.11	32.49	5	0.076
212810669	C6	26.939 ± 0.344	LS	Y	1.418 ± 0.061	4405.41	147.85	6	0.076
212810669	C17	25.721 ± 0.081	LS	Y	1.350 ± 0.600	4551.57	129.93	6	0.092
213817346	C7	0.812 ± 0.004	LS	Y	1.108 ± 0.381	8567.76	918.01	15	0.184
214089305	C7	—	—	N	—	2904.93	137.99	1	0.012
214269391	C7	19.734 ± 0.373	LS	Y	0.158 ± 0.036	831.53	44.03	0	—
214787262	C7	43.307 ± 0.352	LS	?	1.395 ± 0.081	4673.74	103.35	5	0.061
215004972	C7	0.233 ± 0.006	LS	Y	0.072 ± 0.045	554.61	182.32	1	0.012
215632123	C7	2.850 ± 0.021	LS	Y	1.228 ± 0.208	5701.87	765.33	12	0.148
215818496	C7	—	—	N	—	2105.45	76.56	6	0.074
215969058	C7	—	—	N	—	3102.33	53.17	3	0.037
216273315	C7	—	—	N	—	1451.09	63.45	1	0.012

to be continued on the next page

Table A2 continued.

EPIC ID	Camp.	P_{rot} [d]	Method	Flag	R_{per} [%]	S_{ph} [ppm]	S_{flat} [ppm]	N_{Flares}	ν [N_{flares}/d]
216848322	C7	17.280 ± 0.131	LS	Y	0.013 ± 0.577	3308.46	81.52	4	0.049
216892056	C7	69.949 ± 2.915	LS	?	1.870 ± 0.089	6097.17	99.31	2	0.025
218121888	C7	—	—	N	—	7500.18	219.23	4	0.049
218790299	C7	0.902 ± 0.117	LS	Y	0.171 ± 0.036	1440.42	149.75	4	0.049
219448194	C7	—	—	N	—	6781.18	123.93	0	—
220209255	C8	27.652 ± 0.067	LS	Y	0.625 ± 0.128	2920.02	71.75	0	—
220215093	C8	57.550 ± 0.254	LS	?	0.690 ± 0.301	2118.81	120.04	8	0.104
220237354	C8	38.211 ± 0.902	LS	?	1.416 ± 0.066	7242.60	87.45	4	0.052
220256064	C8	16.964 ± 0.034	LS	Y	0.851 ± 0.027	2432.81	61.06	1	0.013
220265960	C8	2.315 ± 0.004	LS	Y	0.402 ± 0.639	5341.84	548.95	5	0.065
220266256	C8	—	—	N	—	1343.11	63.69	0	—
220287795	C8	—	—	N	—	3420.77	81.46	1	0.013
220308656	C8	0.718 ± 0.027	LS	Y	3.144 ± 0.226	18768.14	2054.82	7	0.091
220323325	C8	16.625 ± 0.114	LS	Y	1.252 ± 0.046	4158.88	78.16	0	—
220350328	C8	24.895 ± 0.263	LS	Y	0.655 ± 0.095	3261.56	56.06	0	—
220412416	C8	—	—	N	—	4223.08	64.25	1	0.013
220460555	C8	32.714 ± 0.374	LS	Y	1.278 ± 0.277	4295.59	58.63	0	—
220467322	C8	12.058 ± 0.316	LS	Y	1.408 ± 0.277	5896.78	168.31	5	0.065
220475592	C8	—	—	N	—	3970.20	66.96	4	0.052
220501313	C8	21.296 ± 0.051	LS	?	0.335 ± 0.021	1113.28	48.84	1	0.013
220581451	C8	0.491 ± 0.001	LS	Y	2.347 ± 0.401	17912.05	1848.91	3	0.039
220604532	C8	77.048 ± 3.059	LS	?	1.540 ± 0.359	5528.33	164.84	1	0.013
220611593	C8	29.616 ± 0.594	LS	?	0.430 ± 0.065	1323.57	71.33	2	0.026
220623047	C8	—	—	N	—	1454.54	67.64	2	0.026
220624740	C8	19.026 ± 0.031	LS	Y	1.024 ± 0.078	3956.70	65.38	3	0.039
220676900	C8	—	—	N	—	2038.35	70.02	1	0.013
220677352	C8	9.678 ± 0.052	LS	Y	0.230 ± 0.024	1258.07	67.80	1	0.013
220677738	C8	16.737 ± 0.671	LS	Y	1.379 ± 0.519	5170.08	352.68	7	0.091
220706618	C8	16.964 ± 0.044	LS	Y	0.650 ± 5.189	2025.77	226.82	13	0.169
220732658	C8	38.804 ± 1.077	LS	Y	0.414 ± 0.090	2115.11	97.77	0	—
201077482	C10	23.118 ± 0.702	LS	Y	0.173 ± 0.054	841.74	45.51	2	0.029
201128047	C10	15.222 ± 0.592	ACF	Y	0.195 ± 0.228	909.09	97.04	3	0.043
201223580	C10	54.132 ± 6.238	LS	?	0.759 ± 0.323	4859.63	69.76	3	0.043
201288384	C10	5.413 ± 0.017	LS	Y	5.389 ± 0.466	16968.86	925.26	3	0.043
201296234	C10	11.108 ± 0.776	LS	?	0.090 ± 0.057	915.28	925.26	3	0.043
201416151	C10	12.443 ± 0.145	ACF	Y	3.855 ± 0.178	11877.33	116.27	7	0.101
201431768	C10	38.988 ± 1.247	SINE	?	0.370 ± 0.022	1074.43	48.29	0	—
201506654	C10	1.583 ± 0.013	LS	Y	1.952 ± 0.155	8645.71	1417.57	5	0.072
201530621	C10	46.053 ± 1.242	ACF	?	0.278 ± 0.117	1351.65	132.88	1	0.014
201659529	C10	43.725 ± 1.153	LS	?	0.562 ± 0.507	5995.18	114.75	5	0.072
228711280	C10	60.700 ± 6.070	LS	?	0.657 ± 0.054	2579.52	135.21	0	—
228726301	C10	8.278 ± 0.035	LS	Y	0.317 ± 0.127	2258.41	143.76	6	0.087
228750455	C10	6.721 ± 0.154	LS	Y	0.339 ± 0.047	2028.18	88.50	2	0.029
228757142	C10	—	—	N	—	1351.29	60.04	0	—
228782343	C10	17.469 ± 1.214	LS	Y	0.649 ± 0.024	1704.40	48.93	0	—
228808502	C10	65.465 ± 6.213	LS	?	0.680 ± 0.103	2644.91	81.03	3	0.043
228857363	C10	$77.300 \pm$	SINE	?	0.586 ± 0.133	2646.82	72.93	3	0.043
228858734	C10	—	—	N	—	3731.90	69.30	2	0.029
228861595	C10	40.230 ± 0.869	ACF	?	0.219 ± 0.108	1380.92	48.30	0	—
228864582	C10	0.316 ± 0.000	LS	Y	1.432 ± 0.037	4672.16	2158.84	7	0.101
228885036	C10	18.366 ± 0.191	LS	Y	0.262 ± 0.017	857.71	31.89	0	—
228901441	C10	49.820 ± 1.247	LS	?	0.354 ± 0.060	4160.60	51.66	3	0.043
228972691	C10	—	—	N	—	4609.87	78.18	2	0.029
228982481	C10	—	—	N	—	212.54	78.18	2	0.279
228992431	C10	—	—	N	—	599.82	78.18	2	0.279
229043460	C10	23.946 ± 0.348	ACF	Y	0.266 ± 0.295	2111.45	66.89	1	0.014
229081889	C10	29.018 ± 0.688	LS	Y	1.132 ± 0.140	3094.03	85.15	5	0.072

to be continued on the next page

Table A2 continued.

EPIC ID	Camp.	P_{rot} [d]	Method	Flag	R_{per} [%]	S_{ph} [ppm]	S_{flat} [ppm]	N_{Flares}	ν [N_{flares}/d]
229122988	C10	24.232 ± 1.151	ACF	Y	0.988 ± 0.138	3950.16	76.53	1	0.014
229149393	C10	8.389* ± 0.083	LS	Y	0.199 ± 0.028	559.01	74.27	0	—
223636719	C11	88.533 ±	SINE	?	0.658 ± 0.097	2372.17	106.74	0	—
224945540	C11	37.799 ± 1.273	ACF	?	0.673 ± 0.519	1941.81	108.37	1	0.014
225420708	C11	—	—	N	—	482.91	252.24	0	—
226240066	C11	47.953 ± 0.844	ACF	?	1.528 ± 0.576	2622.69	118.29	2	0.028
229432919	C11	27.759 ± 0.383	SINE	Y	1.852 ± 0.682	3181.53	79.26	0	—
230510723	C11	39.396 ± 4.315	LS	?	0.867 ± 0.130	2515.49	72.25	5	0.069
230751558	C11	—	—	N	1.260 ± 0.531	1117.42	89.35	1	0.014
231116934	C11	34.036 ± 0.141	LS	Y	1.343 ± 0.186	3244.78	85.19	3	0.041
231179480	C11	—	—	N	0.377 ± 0.109	1223.80	72.60	1	0.014
231875643	C11	96.314 ±	SINE	?	5.415 ± 1.700	8088.91	159.10	1	0.014
232017621	C11	—	—	N	—	30878.44	2998.32	6	0.083
232097582	C11	35.995 ± 0.710	LS	Y	0.459 ± 0.032	1419.21	46.82	1	0.014
233488533	C11	78.236 ±	SINE	?	7.097 ± 2.642	8103.40	261.18	3	0.041
234562190	C11	12.929 ± 0.366	LS	Y	35.569 ± 15.033	8394.74	1846.50	1	0.014
234698848	C11	51.059 ± 0.445	ACF	?	0.382 ± 0.104	1111.96	46.70	1	0.014
235067510	C11	40.224 ± 4.022	SINE	?	0.698 ± 0.193	3107.24	71.31	1	0.014
235070897	C11	25.485 ± 0.948	SINE	?	0.378 ± 0.109	1139.61	171.89	0	—
236285338	C11	119.276 ±	SINE	?	0.472 ± 0.102	1591.39	171.89	0	—
236305079	C11	—	—	N	—	384.01	148.16	0	—
236469315	C11	46.543 ± 1.068	ACF	?	0.579 ± 0.068	1671.58	51.82	0	—
237853022	C11	37.062 ± 0.934	LS	?	0.315 ± 0.144	1062.86	136.73	0	—
240451481	C11	—	—	N	—	577.67	197.23	0	—
242219524	C11	23.946 ± 0.221	ACF	Y	0.640 ± 0.241	1631.20	42.36	1	0.014
245919787	C12	5.649 ± 0.016	LS	Y	9.418 ± 2.379	28749.44	992.98	6	0.076
245983914	C12	10.792 ± 0.366	LS	Y	0.795 ± 0.284	2783.65	992.98	6	0.076
246001292	C12	17.641 ± 0.483	LS	Y	0.832 ± 0.258	2276.77	61.55	1	0.013
246001292	C19	17.304 ±	SINE	?	0.423 ± 0.154	1449.13	101.81	2	0.277
246043232	C12	90.667 ±	SINE	?	1.269 ± 0.652	4310.94	104.97	3	0.038
246048874	C12	19.272 ± 0.029	LS	Y	0.677 ± 0.255	2373.47	97.51	3	0.038
246069579	C12	14.588 ± 0.030	ACF	?	0.400 ± 0.129	1201.79	54.22	2	0.025
246132735	C12	105.297 ±	SINE	?	4.717 ± 0.660	16602.57	124.30	5	0.064
246132735	C19	0.687 ± 0.026	LS	Y	0.131 ± 0.015	369.75	65.50	0	—
246159774	C12	36.614 ± 1.324	ACF	?	0.649 ± 2.332	2681.15	476.55	2	0.025
246175846	C12	18.557 ± 0.269	LS	Y	1.359 ± 0.159	4703.55	148.47	1	0.013
246179278	C12	28.491 ± 0.157	LS	Y	5.351 ± 1.885	15660.02	107.42	9	0.114
246179278	C19	—	—	N	—	3204.11	125.40	1	0.139
246191912	C12	—	—	N	—	6686.79	97.75	0	—
246191912	C19	—	—	N	—	593.36	88.52	1	0.139
246215873	C12	106.314 ±	SINE	?	0.808 ± 0.056	2656.73	78.68	2	0.025
246226675	C12	11.079 ± 0.172	LS	Y	0.785 ± 5.679	2021.98	470.67	17	0.216
246238886	C12	33.001 ± 2.632	LS	?	0.312 ± 0.235	910.22	45.85	4	0.051
246238886	C19	—	—	N	—	121.37	29.54	2	0.277
246253313	C12	27.250 ± 0.228	LS	?	2.797 ± 1.084	7119.26	175.30	6	0.076
246301900	C12	4.461 ± 0.118	LS	Y	5.532 ± 0.238	16088.18	721.45	3	0.038
246301900	C19	4.503 ± 0.153	LS	?	9.654 ± 0.334	34565.90	1258.30	0	—
246333864	C12	86.218 ±	SINE	?	2.535 ± 5.487	9744.63	245.26	9	0.114
246333864	C19	—	—	N	—	385.13	296.06	0	—
246338131	C12	17.373* ± 0.637	SINE	?	0.324 ± 0.965	965.50	97.88	1	0.013
246364217	C12	1.908 ± 0.109	LS	Y	1.525 ± 1.187	4500.88	932.20	14	0.178
246364217	C19	1.823 ± 0.063	LS	Y	1.211 ± 0.199	3115.41	855.09	2	0.277
246374497	C12	25.842 ± 0.283	LS	Y	0.776 ± 0.037	2632.06	48.28	8	0.102
246374497	C19	—	—	N	—	1393.15	855.09	2	0.277
246419402	C12	38.017 ± 0.525	LS	?	0.540 ± 0.403	1778.08	75.05	3	0.038
246419402	C19	11.640 ±	SINE	?	0.068 ± 0.108	233.00	57.47	0	—
246461560	C12	42.542 ± 0.742	LS	?	1.286 ± 0.064	4046.02	71.00	1	0.013

to be continued on the next page

Table A2 continued.

EPIC ID	Camp.	P_{rot} [d]	Method	Flag	R_{per} [%]	S_{ph} [ppm]	S_{flat} [ppm]	N_{Flares}	ν [N_{flares}/d]
246461560	C19	11.416 ±	SINE	?	0.132 ± 0.079	418.42	58.17	0	—
210491860	C13	15.031 ± 0.158	LS	Y	1.214 ± 0.221	3509.81	103.61	0	—
210596446	C13	14.424 ± 0.222	LS	Y	1.611 ± 0.300	5031.62	289.07	22	0.276
210653579	C13	15.122 ± 0.072	LS	Y	2.021 ± 0.125	6929.34	69.39	2	0.025
210721261	C13	1.540 ± 0.014	LS	Y	20.061 ± 3.740	64257.52	6736.44	1	0.013
210840804	C13	0.849 ± 0.000	SINE	?	2.978 ± 3.870	8276.73	776.85	18	0.226
210889984	C13	11.558 ± 0.042	LS	Y	2.651 ± 0.294	7902.54	83.84	4	0.050
210895913	C13	—	—	N	—	1813.38	93.88	0	—
210915518	C13	36.246 ± 1.242	ACF	Y	1.789 ± 0.465	5135.82	91.38	1	0.013
246625561	C13	2.215 ± 0.041	LS	?	9.668 ± 3.023	29923.52	3480.72	5	0.063
246732310	C13	12.933 ± 0.047	LS	Y	3.944 ± 0.149	12737.03	167.02	28	0.352
246774176	C13	2.541 ± 0.005	LS	Y	1.671 ± 10.210	4897.84	1193.52	16	0.201
246806983	C13	2.605 ± 0.053	LS	Y	3.301 ± 0.740	11675.15	919.54	6	0.075
246807434	C13	107.122 ±	SINE	?	0.990 ± 0.046	3360.50	79.69	0	—
246812637	C13	—	—	N	—	3533.78	147.89	0	—
246818597	C13	6.518 ± 0.620	ACF	?	1.343 ± 0.524	4009.26	61.62	4	0.050
246849411	C13	—	—	N	—	705.07	215.23	0	—
246862801	C13	15.992 ± 0.080	LS	Y	1.797 ± 0.214	5966.60	70.57	3	0.038
246931087	C13	10.809 ± 0.139	LS	Y	1.810 ± 0.406	5246.94	122.14	12	0.151
247003390	C13	28.944 ± 0.224	LS	?	0.845 ± 0.097	2437.04	69.07	2	0.025
247080522	C13	44.333 ± 4.433	LS	?	1.626 ± 0.167	5239.93	103.66	2	0.025
247094343	C13	21.672 ± 0.393	LS	Y	1.959 ± 0.044	6336.66	111.51	9	0.113
247122957	C13	1.546 ± 0.008	LS	Y	8.959 ± 2.013	21079.30	2549.57	6	0.075
247130198	C13	—	—	N	—	72991.96	34587.19	0	—
247164626	C13	21.303 ± 0.318	LS	Y	1.874 ± 0.597	5514.76	137.12	11	0.138
247191714	C13	—	—	N	—	5188.62	110.15	1	0.013
247238215	C13	20.636 ± 0.154	ACF	Y	2.012 ± 0.300	5947.41	55.50	4	0.050
247269565	C13	14.852 ± 0.166	LS	Y	1.894 ± 0.635	5872.04	417.07	17	0.214
247282522	C13	1.460 ± 0.041	LS	?	2.593 ± 0.949	9392.35	250.91	5	0.063
247289039	C13	5.950 ± 0.039	LS	Y	2.040 ± 0.423	6379.93	711.76	26	0.327
247309641	C13	0.342 ± 0.002	LS	Y	6.824 ± 1.131	20540.71	8702.20	1	0.013
247325547	C13	16.163 ± 1.616	SINE	?	0.414 ± 0.079	1403.84	42.69	3	0.038
247449449	C13	19.180 ± 0.254	LS	Y	2.054 ± 4.267	6232.58	200.39	13	0.163
247476655	C13	9.149 ± 0.033	LS	Y	3.325 ± 0.199	10025.91	171.03	14	0.176
247514292	C13	27.973 ± 0.177	LS	?	0.994 ± 0.069	2847.29	74.88	1	0.013
247592661	C13	2.498 ± 0.103	LS	Y	6.717 ± 6.602	22203.97	2012.33	7	0.088
247640857	C13	27.583 ± 1.025	ACF	Y	0.506 ± 0.077	1503.78	58.73	0	—
247657761	C13	79.602 ±	LS	?	0.204 ± 0.040	747.48	49.98	0	—
247679710	C13	27.973 ± 1.728	LS	Y	1.193 ± 0.318	3520.04	71.36	0	—
247725508	C13	19.034 ± 0.193	LS	Y	0.446 ± 0.312	1419.88	73.17	1	0.013
247730793	C13	108.067 ±	SINE	?	0.210 ± 0.314	642.34	73.17	1	0.013
247734588	C13	63.450 ± 0.295	LS	?	0.466 ± 0.197	1545.80	112.09	3	0.038
247744104	C13	16.304 ± 0.107	LS	Y	0.986 ± 0.079	3268.97	60.59	2	0.025
247827225	C13	30.484 ± 0.691	ACF	Y	0.703 ± 0.122	2013.73	60.59	2	0.025
247867687	C13	20.433 ± 0.180	LS	Y	0.451 ± 0.146	1522.30	50.37	1	0.013
247905449	C13	36.032 ± 1.822	LS	?	0.684 ± 0.240	2140.84	67.82	0	—
247909274	C13	46.823 ± 1.850	LS	?	1.348 ± 0.230	4349.17	114.88	6	0.075
247969864	C13	31.495 ± 0.226	LS	Y	1.003 ± 0.040	3297.30	50.96	0	—
247983269	C13	46.823 ± 0.905	LS	?	0.938 ± 0.191	2864.10	116.55	2	0.025
247988033	C13	19.787 ± 0.249	LS	Y	0.357 ± 0.101	1364.37	98.88	0	—
248030935	C13	61.275 ± 0.655	ACF	?	0.097 ± 0.360	311.86	119.75	1	0.013
248042336	C13	87.640 ±	SINE	?	1.070 ± 0.393	3234.05	79.10	0	—
201497396	C14	13.590 ± 0.173	LS	Y	0.707 ± 0.073	2200.24	88.97	14	0.180
201501470	C14	1.304 ± 0.045	LS	Y	9.672 ± 3.210	31145.24	2052.62	7	0.090
201661761	C14	84.097 ±	SINE	?	0.534 ± 0.916	1916.39	155.35	0	—
201703096	C14	21.367 ± 0.216	LS	Y	1.261 ± 0.164	3793.91	87.13	1	0.013
201705990	C14	29.754 ± 0.130	LS	Y	1.424 ± 0.070	4243.25	104.49	11	0.141

to be continued on the next page

Table A2 continued.

EPIC ID	Camp.	P_{rot} [d]	Method	Flag	R_{per} [%]	S_{ph} [ppm]	S_{flat} [ppm]	N_{Flares}	ν [N_{flares}/d]
201820874	C14	1.107 ± 0.000	LS	Y	6.993 ± 1.883	18021.67	3030.69	2	0.026
248425357	C14	108.485 ±	SINE	?	0.849 ± 0.126	3072.95	113.42	2	0.026
248432941	C14	30.479 ± 0.057	LS	?	0.476 ± 0.162	1468.13	37.05	20	0.256
248453031	C14	34.232 ± 0.895	LS	Y	1.014 ± 0.067	3415.96	50.69	6	0.077
248468115	C14	3.528 ± 0.001	LS	Y	1.447 ± 0.292	4382.01	330.16	9	0.115
248473036	C14	0.708 ± 0.000	LS	Y	2.977 ± 0.379	8774.53	1790.97	4	0.051
248504645	C14	41.640 ± 0.173	LS	?	0.654 ± 0.200	1987.30	55.74	0	—
248505702	C14	21.453 ± 0.209	ACF	Y	0.410 ± 0.090	1215.92	41.01	2	0.026
248601792	C14	0.692 ± 0.000	LS	Y	4.015 ± 0.698	12003.81	3744.08	14	0.180
248637069	C14	56.004 ± 1.402	ACF	?	1.303 ± 0.157	4138.97	43.23	15	0.192
248664460	C14	26.311 ± 2.631	LS	?	0.836 ± 0.260	2935.46	57.41	0	—
248698478	C14	—	—	N	—	1857.63	59.08	2	0.026
248759329	C14	97.473 ±	SINE	?	0.887 ± 0.217	3014.70	83.39	4	0.051
248775337	C14	58.353 ± 5.835	ACF	?	1.163 ± 0.477	3726.03	98.28	0	—
248804846	C14	20.161 ± 0.330	LS	Y	0.670 ± 0.018	2198.63	46.19	0	—
248826058	C14	59.453 ± 0.225	LS	?	1.161 ± 0.540	3762.75	118.50	0	—
248849485	C14	18.658 ± 0.056	LS	Y	0.950 ± 0.173	3074.94	83.62	1	0.013
248856749	C14	0.452 ± 0.001	LS	Y	8.610 ± 3.744	26470.20	7042.41	0	—
248857979	C14	16.236* ± 0.478	LS	Y	0.625 ± 0.174	1834.36	50.30	1	0.013
248870284	C14	57.005 ± 2.204	ACF	?	1.382 ± 0.494	4305.31	107.04	4	0.051
249101965	C15	66.301 ± 1.081	ACF	?	0.952 ± 0.378	2959.16	154.12	1	0.012
249186244	C15	—	—	N	—	3747.36	147.21	0	—
249328859	C15	—	—	N	—	36870.70	1664.57	0	—
249338840	C15	22.354 ± 0.081	LS	Y	0.569 ± 0.062	1780.87	66.12	6	0.069
249591902	C15	29.814 ± 0.050	LS	Y	1.415 ± 0.396	4697.11	99.56	5	0.058
249655888	C15	16.305 ± 0.293	ACF	Y	0.694 ± 0.285	2165.30	99.56	5	0.058
249677429	C15	3.927 ± 0.029	LS	Y	5.250 ± 1.040	15507.49	855.78	15	0.173
249680584	C15	3.897 ± 0.015	LS	Y	1.641 ± 0.361	4787.26	521.88	7	0.081
249681555	C15	—	—	N	—	3210.92	48.26	1	0.012
249860217	C15	41.073 ± 0.216	LS	?	0.443 ± 0.062	1454.46	49.69	0	—
249899499	C15	31.306 ± 1.558	LS	?	0.696 ± 0.248	1941.06	94.93	1	0.012
250022000	C15	20.520 ± 1.001	LS	Y	0.279 ± 0.077	775.21	70.93	1	0.012
250034723	C15	16.913 ± 0.057	LS	Y	1.185 ± 0.170	3640.67	54.17	1	0.012
250053801	C15	17.673 ± 0.924	ACF	Y	1.237 ± 0.317	3608.72	87.28	0	—
250072828	C15	78.410 ± 0.562	LS	?	0.828 ± 0.075	2618.98	103.18	0	—
250111823	C15	69.674 ± 0.342	LS	?	1.073 ± 0.116	3605.33	69.56	0	—
250122612	C15	41.073 ± 1.327	LS	?	0.447 ± 0.066	1379.45	78.01	1	0.012
211400445	C16	32.018 ± 0.562	LS	Y	0.858 ± 0.028	2590.53	52.91	3	0.039
211456957	C16	38.409 ± 0.240	LS	Y	0.802 ± 0.226	2555.51	45.98	0	—
211467243	C16	0.263 ± 0.001	LS	Y	1.583 ± 0.708	4576.92	1936.12	1	0.013
211489708	C16	31.512 ± 2.105	ACF	Y	1.056 ± 0.253	3241.73	75.73	0	—
211516815	C16	30.755 ± 0.980	ACF	Y	1.238 ± 0.075	3715.82	73.90	2	0.026
211616023	C16	19.833 ± 1.214	LS	Y	0.639 ± 0.167	2002.47	61.99	0	—
211630934	C16	19.524 ± 0.294	LS	Y	0.288 ± 0.040	869.23	32.52	0	—
211736506	C16	26.137 ± 0.063	ACF	?	0.227 ± 0.021	666.34	28.67	0	—
211832386	C16	—	—	N	—	5756.17	94.75	2	0.026
211857745	C16	—	—	N	—	3696.66	40.75	2	0.026
211864396	C16	57.925 ± 0.678	SINE	?	1.579 ± 0.046	4972.43	70.36	3	0.039
211890761	C16	14.785 ± 0.054	SINE	?	2.870 ± 1.635	10181.54	62.57	2	0.026
212038542	C16	26.023 ± 0.368	LS	Y	0.262 ± 0.142	742.60	57.61	0	—
212093841	C16	51.976 ± 2.130	LS	?	0.449 ± 0.289	1344.17	77.74	0	—
251282832	C16	74.879 ± 1.029	SINE	?	0.710 ± 0.292	2491.22	122.99	2	0.026
251341401	C16	29.775 ± 0.009	ACF	Y	1.384 ± 0.140	4317.59	60.84	2	0.026
212518679	C17	34.146 ± 0.143	LS	?	0.604 ± 0.041	1707.99	72.75	0	—
212610229	C17	31.561 ± 0.182	LS	Y	0.679 ± 0.679	2081.54	104.36	0	—
212652474	C17	28.026 ± 0.440	LS	Y	0.893 ± 0.062	2818.94	71.08	1	0.015
212662886	C17	37.213 ± 0.192	ACF	?	0.545 ± 0.087	1721.54	63.60	2	0.031

to be continued on the next page

Table A2 continued.

EPIC ID	Camp.	P_{rot} [d]	Method	Flag	R_{per} [%]	S_{ph} [ppm]	S_{flat} [ppm]	N_{Flares}	ν [N_{flares}/d]
212712579	C17	27.114 ± 2.711	LS	?	1.290 ± 0.435	3428.65	51.15	0	—
212734783	C17	$73.819 \pm$	SINE	?	0.826 ± 0.085	2630.61	67.52	0	—
212840848	C17	—	—	N	—	1133.34	27.94	2	0.031
212846068	C17	19.972 ± 0.053	LS	Y	0.415 ± 0.015	1334.66	47.90	0	—
212874829	C17	30.410 ± 0.951	LS	Y	1.359 ± 0.596	4289.12	94.78	7	0.107
251512053	C17	31.168 ± 0.924	LS	Y	0.517 ± 0.054	1413.21	54.22	0	—
251540467	C17	14.632 ± 0.844	ACF	?	1.140 ± 0.414	3491.52	61.23	1	0.015
251550724	C17	46.965 ± 0.134	LS	?	1.178 ± 0.048	3677.56	40.36	7	0.107
251567386	C17	—	—	N	—	3657.93	132.35	0	—
251583820	C17	52.926 ± 0.256	LS	?	0.600 ± 0.128	2009.39	137.12	0	—
251584738	C17	41.648 ± 1.080	ACF	?	0.891 ± 0.082	2607.61	50.08	1	0.015
211944670	C18	2.773 ± 0.015	SINE	Y	3.986 ± 3.815	9964.50	1708.36	6	0.122
246033148	C19	4.662 ± 0.084	LS	?	3.182 ± 0.620	9970.91	1095.10	1	0.139
246079058	C19	$9.005 \pm$	SINE	?	0.061 ± 0.038	185.44	1095.10	1	0.138
246093819	C19	—	—	N	—	315.56	65.50	0	—
246141580	C19	—	—	N	—	828.37	237.00	3	0.416
246182783	C19	3.774 ± 0.317	LS	?	0.043 ± 0.011	130.69	125.40	1	0.139
246310210	C19	$13.281 \pm$	SINE	?	0.156 ± 0.041	463.71	1258.30	0	—
246378594	C19	—	—	N	—	668.61	93.17	1	0.139
246379501	C19	$8.699 \pm$	SINE	?	0.876 ± 0.030	2979.04	57.47	0	—
246424810	C19	—	—	N	—	126.31	76.20	0	—
246446811	C19	—	—	N	—	8145.32	265.33	1	0.139
251718998	C19	0.415 ± 0.003	LS	Y	1.619 ± 0.118	4881.10	58.17	0	—
251728337	C19	$10.534 \pm$	SINE	?	0.192 ± 0.006	720.72	37.75	0	—

* P_{rot} could be twice the given value.

B Multiplicity of the stars in the K2 M-dwarf sample

Table B1: Multiplicity status for our targets. We list here visual as well as close eclipsing and spectroscopic binaries. In total, we found 96 possible binaries or multiple systems.

EPIC ID	Camp.	Name	Component	Separation [arcsec]
202059183	C0	Gaia DR2 3423743492225744128		7.2
202059188	C0	WDS 06102+2234		1.9
202059198	C0	WDS 06215+1618		115.0
202059199	C0	Gaia DR2 3369198983818682624		119.0
202059221	C0	WDS 06401+2835		0.3
201367065	C1	WDS 11293-0127		26.0
201481218	C1	WDS 11132+0014		0.2
201482319	C1	WDS 11477+0016		24.7
201497866	C1	WDS 11428+0029		25.8
201506253	C1	WDS 11321+0038		34.2
201718613	C1	WDS 11522+0357		0.3
201909533	C1	WDS 11519+0731		0.5
202571062	C2	WDS 16240-2911		6.2
203099398	C2	WDS 16153-2716		2.0
203124214	C2	WDS 16254-2710		3.0
204976998	C2	UCAC4 351-084361		7.6
205030726	C2	WDS 16475-1945		196.6
205467732	C2	WDS 16268-1724		0.7
205952383	C3	WDS 22365-1618		7.3
206007536	C3	WDS 22526-1437		6.5
206055065	C3	WDS 22291-1316		230.4
206107346	C3	WDS 22059-1155		
206181550	C3	WDS 22118-1005		204.4

to be continued on the next page

Table B1 continued.

EPIC ID	Camp.	Name	Component	Separation [arcsec]
206208968	C3	WDS 22334-0937		1.5
206262223	C3	WDS 22173-0847	AB	7.9
206262223	C3	WDS 22173-0847	AC	2.6
206262223	C3	WDS 22173-0847	Ba,Bb	0.5
206262336	C3	WDS 22173-0847	AB	7.9
206262336	C3	WDS 22173-0847	AC	2.6
206262336	C3	WDS 22173-0847	Ba,Bb	0.5
210408563	C4	WDS 04178+1340		0.8
210434769	C4	WDS 04077+1413		159.5
210434976	C4	WDS 03510+1414		28.8
210489654	C4	WDS 04207+1514		0.2
210579749	C4	Gaia DR2 0043335537119008896		111.1
210580056	C4	WDS 03439+1640	AB	106.5
210580056	C4	WDS 03439+1640	AC	79.6
210580056	C4	WDS 03439+1640	AD	127.5
210613397	C4	WDS 03462+1710		14.1
210651981	C4,C13	WDS 04285+1742		1.6
211036776	C4	WDS 04087+2333		1.7
211385897	C5,C18	WDS 08290+1125		
211788733	C5,C18	WDS 08211+1710		32.3
211944676	C5,C18	WDS 08317+1924	Aa,Ab	0.9
211944676	C5,C18	WDS 08317+1924	AB	10.0
211944676	C5,C18	WDS 08317+1924	AC	21.5
211944676	C5,C18	WDS 08317+1924	Ba,Bb	0.4
211944856	C5,C18	WDS 08317+1924	Aa,Ab	0.9
211944856	C5,C18	WDS 08317+1924	AB	10.0
211944856	C5,C18	WDS 08317+1924	AC	21.5
211944856	C5,C18	WDS 08317+1924	Ba,Bb	0.4
212329328	C6	WDS 13515-1641	AB	6.8
212329328	C6	WDS 13515-1641	AC	6.4
212647740	C6	WDS 14020-0930		
212679181	C6,C17	WDS 13269-0846		1.3
212710520	C6,C17	Gaia DR2 3630359628505968640		31.5
212810669	C6,C17	WDS 13434-0513		8.2
213817346	C7	WDS 19279-2811		0.9
215632123	C7	WDS 18498-2350	AB	6.2
215632123	C7	WDS 18498-2350	AC	8.3
215969058	C7	WDS 19153-2313		5.8
220215093	C8	WDS 01227+0032		1.8
220350328	C8	WDS 00389+0342		0.8
220412416	C8	Gaia DR2 2552102419488768512		86.7
220460555	C8	WDS 00443+0554		1.5
220623047	C8	WDS 01025+0933		28.9
220676900	C8	Gaia DR2 2583179080560149248		21.2
220677738	C8	WDS 00503+1052		41.7
201659529	C10	WDS 12169+0258		2.1
228750455	C10	WDS 12089-0854		1.4
228757142	C10	WDS 12478-0836		4.9
228864582	C10	WDS 12228-0405	AB	0.2
228864582	C10	WDS 12228-0405	AC	5.4
228864582	C10	WDS 12228-0405	AD	4.4
228901441	C10	WDS 12277-0315		1.5
229043460	C10	Gaia DR2 3696387599561169408		24.9
229081889	C10	Gaia DR2 3696918771053032704		2.8
229122988	C10	WDS 12289+0122		85.1
230751558	C11	WDS 17080-1929		2.5
232097582	C11	WDS 17021-2718		14.5
234562190	C11	WDS 17132-1834	AB	3.2

to be continued on the next page

Table B1 continued.

EPIC ID	Camp.	Name	Component	Separation [arcsec]
234562190	C11	WDS 17132-1834	AC	3.5
234698848	C11	Gaia DR2 4110661144000540160		3.9
242219524	C11	WDS 17378-2959		1.8
246159774	C12	WDS 23106-0550		10.1
246238886	C12,C19	WDS 23073-0416		7.5
246364217	C12,C19	WDS 23210-0148		0.1
210840804	C13	WDS 04216+2029	Aa,Ab	1.2
210840804	C13	WDS 04216+2029	AB	113.6
246931087	C13	TYC 1284-1056-1		SB
247449449	C13	WDS 04390+2149	AB	15.0
247449449	C13	WDS 04390+2149	AC	1.2
247905449	C13	WDS 05003+2508	BC	39.2
247988033	C13	WDS 04308+2543		138.9
201703096	C14	WDS 11008+0342		3.0
201820874	C14	WDS 10572+0545		1.0
248504645	C14	WDS 10428+0317		2.1
248601792	C14	WDS 10523+0555		26.7
248637069	C14	WDS 10509+0648	AB	12.5
248637069	C14	WDS 10509+0648	AC	13.9
248775337	C14	WDS 10403+1005		86.2
249681555	C15	L 768-119		SB
250022000	C15	WDS 15256-1513		7.7
250034723	C15	WDS 15236-1504		6.8
250072828	C15	WDS 15496-1437		40.4
211400445	C16	WDS 08571+1139		0.7
211456957	C16	WDS 08548+1230		2.4
211467243	C16	WDS 08563+1239		1.8
211616023	C16	Gaia DR2 0606742406339556480		3.3
211736506	C16	WDS 09045+1625		4.1
212093841	C16	WDS 09080+2154		0.1
212518679	C17	WDS 13232-1220		304.8
251550724	C17	WDS 13283-0222		8.5
251583820	C17	WDS 13203-0140	BD	35.5
251584738	C17	WDS 13203-0140	AB	199.8
251584738	C17	WDS 13203-0140	AC	135.3
211944670	C18	WDS 08317+1924	Aa,Ab	0.9
211944670	C18	WDS 08317+1924	AB	10.0
211944670	C18	WDS 08317+1924	AC	21.5
211944670	C18	WDS 08317+1924	Ba,Bb	0.4

C Example light curves

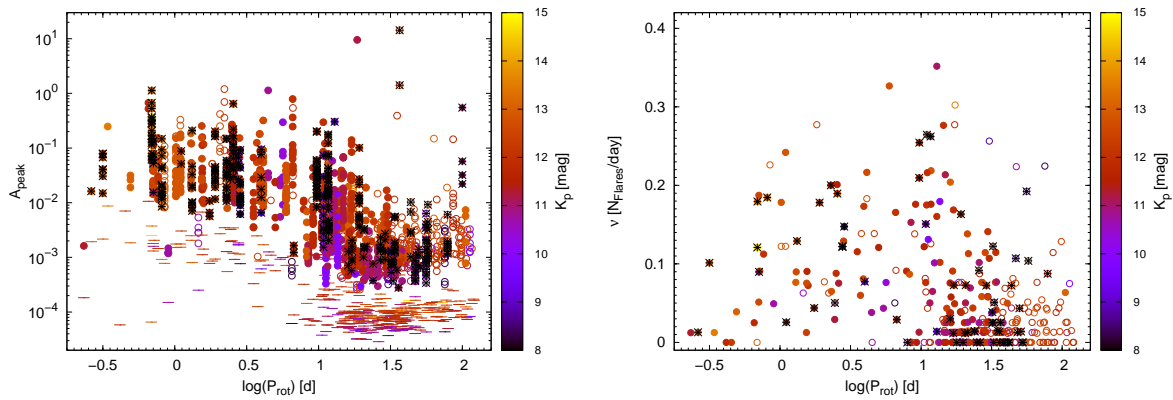


Fig. B1 Relation between rotation period and activity indicators related to flares for all 341 targets with measurable rotation period. Full and open symbols denote reliable periods and periods with less confidence, respectively. The black crosses mark the multiple systems that were explained in detail in Section 2.2.

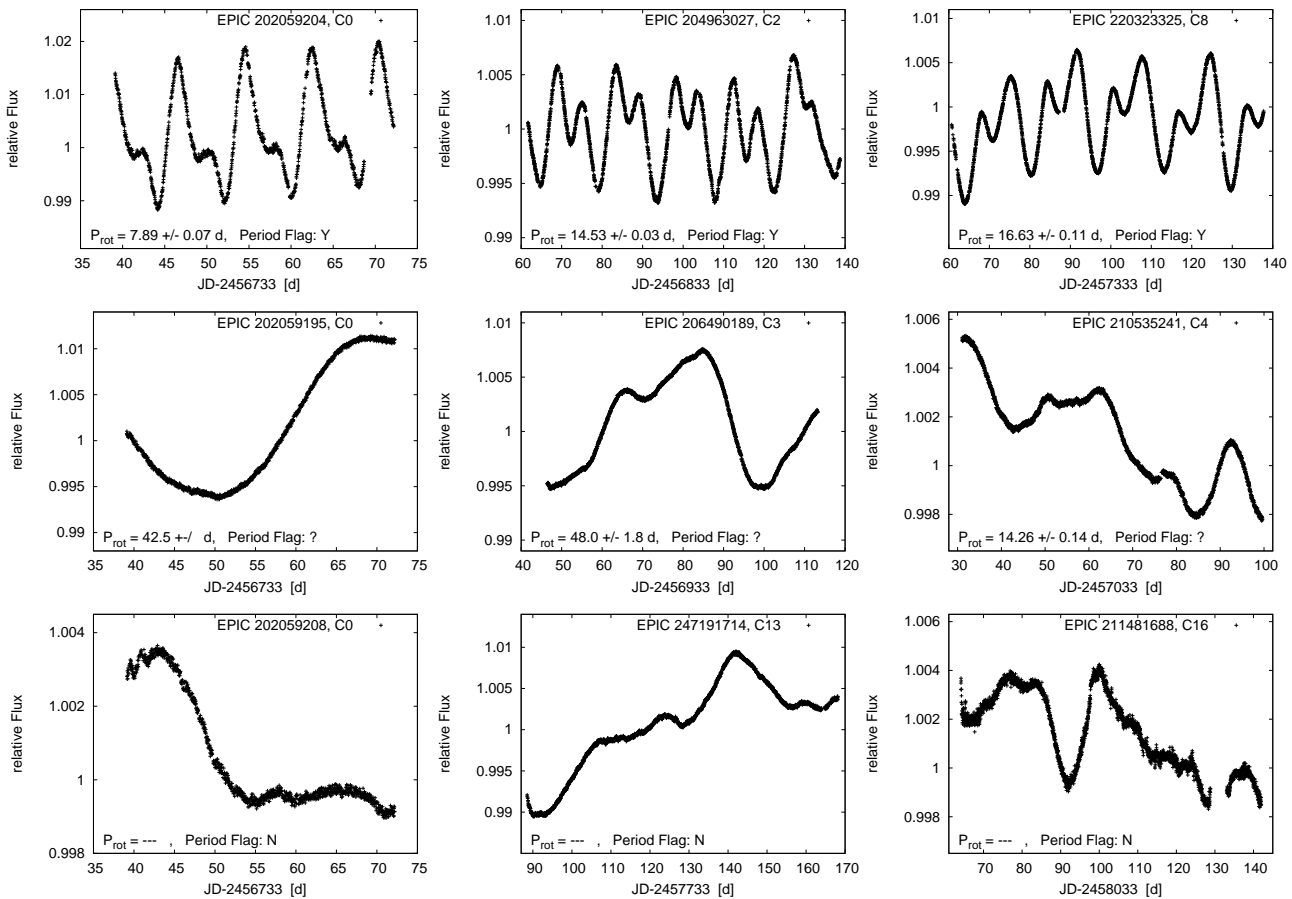


Fig. C1 Various LCs that represent examples for the different period flags. The different rows show, from top to bottom, stars with an reliable period estimate (flag ‘Y’), stars with periods with lower confidence (flag ‘?’) and stars with no detected period (flag ‘N’).